Received: 26 July 2023 | Revised: 25 December 2023 | Accepted: 28 January 2024

DOI: 10.1002/ajpa.24915

RESEARCH ARTICLE

AMERICAN JOURNAL OF BIOLOGICAL ANTHROPOLOGY

WILEY

Quantifying hominin morphological diversity at the end of the middle Pleistocene: Implications for the origin of *Homo sapiens*

Hugo Hautavoine[1] | Julie Arnaud[1,2] | Antoine Balzeau[1,3] | Aurélien Mounier[1,4]

[1]PaléoFED, Histoire Naturelle de l'Homme Préhistorique (HNHP, UMR 7194), MNHN/CNRS/UPVD, Paris, France

[2]Dipartimento di Studi Umanistici, Università degli Studi di Ferrara, Ferrara, Italy

[3]Département de Zoologie Africaine, Musée Royal de l'Afrique Centrale, Tervuren, Belgium

[4]Turkana Basin Institute, Nairobi, Kenya

Correspondence
Hugo Hautavoine, Histoire Naturelle de l'Homme Préhistorique (HNHP, UMR 7194), MNHN/CNRS/UPVD, Musée de l'Homme, Paris, France.
Email: hugo.hautavoine@edu.mnhn.fr

Abstract

Objectives: The Middle Pleistocene (MP) saw the emergence of new species of hominins: *Homo sapiens* in Africa, *H. neanderthalensis*, and possibly Denisovans in Eurasia, whose most recent common ancestor is thought to have lived in Africa around 600 ka ago. However, hominin remains from this period present a wide range of morphological variation making it difficult to securely determine their taxonomic attribution and their phylogenetic position within the *Homo* genus. This study proposes to reconsider the phenetic relationships between MP hominin fossils in order to clarify evolutionary trends and contacts between the populations they represent.

Materials and Methods: We used a Geometric Morphometrics approach to quantify the morphological variation of the calvarium of controversial MP specimens from Africa and Eurasia by using a comparative sample that can be divided into 5 groups: *H. ergaster*, *H. erectus*, *H. neanderthalensis*, and *H. sapiens*, as well as individuals from current modern human populations. We performed a Generalized Procrustes Analysis, a Principal Component Analysis, and Multinomial Principal Component Logistic Regressions to determine the phenetic affinities of the controversial Middle Pleistocene specimens with the other groups.

Results: MP African and Eurasian specimens represent several populations, some of which show strong affinities with *H. neanderthalensis* in Europe or *H. sapiens* in Africa, others presenting multiple affinities.

Discussion: These MP populations might have contributed to the emergence of these two species in different proportions. This study proposes a new framework for the human evolutionary history during the MP.

KEYWORDS

calvarium, geometric morphometrics, *Homo sapiens* origin, late middle Pleistocene, multinomial logistic regression

1 | INTRODUCTION

The evolutionary history of hominin populations during the Middle Pleistocene (MP) (i.e., Chibanian, 0.77–0.126 Ma) has generated numerous debates within the scientific community (Stringer, 2002; Rightmire, 2008; Mounier et al., 2009; Tattersall, 2011). This period saw, around 250 ka, the emergence of *Homo neanderthalensis* in Europe, *H. sapiens* in Africa, and possibly Denisovans (Reich et al., 2010) in Asia,

whose most recent common ancestor is thought to have lived in Africa about 600 ka (Meyer et al., 2016; Mounier & Mirazón Lahr, 2016; Schlebusch et al., 2017).

The shift to a 100-ka climate cycle during the MP implied a greater amplitude in the climatic conditions between interglacial and glacial periods, which seems to have favored the mobility of hominin populations (Bräuer, 2008; Lahr & Foley, 1998). These periods of highly contrasting climate might be at the origin of important demographic discontinuities in Eurasia, marked by episodes of northward migration during interglacials, and glacial periods during which only the populations in southern Eurasia and the Levant would have survived (Dennell, 2008; Dennell et al., 2011). In Africa, long humid periods from approximately 620 to 460 ka and from 400 to 160 ka were alternating with shorter arid episodes from about 450 to 400 ka and from 270 to 250 ka (Duesing et al., 2021). Therefore, episodes of expansions might also have been driven by climatic and ecological factors and could have favored interactions between hominin populations within and outside the continent (deMenocal, 2011; Mirazón Lahr, 2016). This could partly explain the high degree of morphological variation that can be observed in the hominin fossil record of this period. These specimens exhibit mosaics of morphological features, which are variably interpreted by palaeoanthropologists, hindering the establishment of a consensus taxonomy and phylogeny (Arsuaga et al., 2014; Di Vincenzo & Manzi, 2023; Hublin, 2001; Mounier & Caparros, 2015; Stringer, 1983). The debate within the scientific community focuses mostly on two conflicting hypotheses (1) the existence of two distinct species (i.e., *H. heidelbergensis* in Europe and *H. rhodesiensis* in Africa), where *H. heidelbergensis* is a chronospecies of *H. neanderthalensis* and *H. rhodesiensis* an exclusive ancestor of *H. sapiens* (Arsuaga et al., 1997); and (2) a unique species present in Africa and Europe (i.e., *H. heidelbergensis s.l.*), ancestral to both species (Mounier, 2009, 2011; Rightmire, 1998). Nevertheless, some late MP fossils can be easily classified either as *H. sapiens* (i.e., Omo I) or *H. neanderthalensis* (i.e., Saccopastore 1). Other specimens, such as the fossils from Jebel Irhoud, are more difficult to classify, given their mosaic morphology retaining characters shared with more basal taxa (i.e., *H. ergaster* and *H. erectus*) along with sapiens-like features (Hublin et al., 2017). Similarly, the specimens from Sima de los Huesos, though being dated to about 427 ka (Arnold et al., 2014), are often presented as the first representatives of *H. neanderthalensis* (Arsuaga et al., 2014; Mounier & Caparros, 2015). Moreover, several genetic studies (Meyer et al., 2016; Petr et al., 2020; Posth et al., 2017) have highlighted the existence of contacts between African and Eurasian hominin populations during Late Middle Pleistocene (LMP, from 350 to 130 ka). These new genomic data, along with new fossil and chronological evidence suggest a more complex pattern than previously thought for human evolution during the MP.

The present study proposes to reconsider the phenetic relationships between MP specimens in order to decipher evolutionary trends and possible contacts between the populations that those fossils represent. To this end, we performed a Geometric Morphometrics analysis to quantify the morphological variation of the calvarium of the hominins from this period to the exclusion of well-classified individuals (i.e., Omo 1, Saccopastore 1). Our study sample is composed of controversial African and Eurasian MP fossil crania. Our comparative sample consists of specimens divided into *H. ergaster*, *H. erectus*, *H. neanderthalensis*, Pleistocene *H. sapiens*, as well as Holocene Africans and Europeans. We performed a Generalized Procrustes Analysis (GPA), a Principal Component Analysis (PCA), and, for the first time in this context, Multinomial Principal Component Logistic Regressions using neural network (MLR) to quantify the phenetic affinities of each Middle Pleistocene hominin with the groups forming the comparative sample. We aim to test the following hypotheses:

1. African and Eurasian MP specimens present different phenetic affinities which are linked to a separate phylogenetic history. This would suggest a separate evolutionary history between two separated lineages, ancestral to *H. neanderthalensis* and possibly Denisovans in Eurasia and to *H. sapiens* in Africa
2. Phenetic affinities of MP fossils are not congruent with geography indicating a more complex evolutionary history. Several populations might have lived contemporaneously at the continental level, suggesting that they might have contributed to the apparition of *H. neanderthalensis* and *H. sapiens* in different proportions.
3. Phenetic affinities of MP fossils are not congruent with chronology. It would suggest that Middle Pleistocene hominins did not follow an anagenetic evolution and that the origins of *H. neanderthalensis* and *H. sapiens* are speciation events.

2 | MATERIALS AND METHODS

The sample analyzed in the present study is composed of 67 3D calvaria divided into a study sample ($n = 14$) and a comparative sample ($n = 53$). The study sample is formed of MP African (n = 8) and Eurasian ($n = 6$) fossils which are not attributed to a consensually defined taxon (Table 1). The comparative sample includes 53 specimens divided into 5 groups (Table 1): 5 Early Pleistocene specimens from continental Africa and Georgia, grouped as *H. ergaster* (Lordkipanidze et al., 2013); 10 *H. erectus* from continental and insular Asia; 11 *H. neanderthalensis*; 14 Pleistocene *H. sapiens* specimens from Africa and Europe, and 15 Holocene individuals (i.e., 11 Africans and 4 Europeans). The Holocene group is used to provide a measure of current adult human variation from Africa and Europe, with a sex ratio composed of 7 females and 8 males. The number of specimens was kept low to emulate the number of specimens in the fossil groups. More African individuals than Europeans were added as they present more genetic variation (Schlebusch et al., 2020).

Different imaging techniques were used to study the 3D calvaria: (1) medical computed tomographic scans (CT; voxel size between 0.449219 and 0.488281 mm) processed with the Amira software (v.5.5, FEI); (2) photogrammetry (PH) with Photoscan (Agisoft, v.1.2.6), and (3) 3D surface scans (OP), obtained with an optical scanner (HDI Advance, 45 µ accuracy), using the FlexScan 3D software (v.3.3, LMI). Photogrammetry, laser surface scanning, and medical computed tomographic scans produce reliable 3D models with a comparable error

TABLE 1 Specimens included in the study.

Specimen	Site	Chronology	Reference	Institution	3D model
Study sample					
Eurasian specimens					
Petralona	Petralona, Greece	150–250 ka (?)	Grün, 1996	GPUT	PH
SH5	Sima de los Huesos, Atapuerca, Spain	427 ± 12 ka	Arnold et al., 2014	FD	PH
Ceprano	Ceprano, Italy	385–430 ka	Manzi et al., 2010	SU	CT
Jinniushan	Jinniu Shan, Liaoning, China	~260 ka	Rosenberg et al., 2006	FD	PH
Dali	Dali, Shaanxi, China	~270 ka	Xiao et al., 2002	IPH	PH
Narmada	Narmada river, Madhya Pradesh, India	150–200 ka (?)	Kennedy, 2014	FD	PH
African specimens					
Saldanha	Elandsfontein, South Africa	~600 ka (?)	Klein et al., 2007	IMCT	OP
Kabwe 1	Kabwe, Zambia	299 ka ± 25 ka	Grün et al., 2020	MH	PH
Ndutu	Ndutu, Tanzania	200–400 ka (?)	Rightmire, 1983	IPH	PH
LH 18	Laetoli, Tanzania	200–300 ka	Manega, 1995	TAZ	CT
KNM-ES 11693	Eliye Springs, Kenya	270–300 ka	Bräuer et al., 2003	NMK	PH
Irhoud 1	Jebel Irhoud, Morocco	315 ± 34 ka	Richter et al., 2017	IPH	PH
Irhoud 2	id.	id.	id.	IPH	PH
Omo II	Omo Kibish, Ethiopia	~230 ka (?)	Vidal et al., 2022	NMK	PH
Comparative sample					
Homo ergaster					
KNM-ER 3733	Koobi Fora, Kenya	~1.63 Ma	Lepre & Kent, 2015	NMK	PH
KNM-ER 3883	id.	1.6–1.5 Ma	id.	NMK	PH
OH 9	Oduvai Gorge, Tanzania	~1.4 Ma	Tamrat et al., 1995	TAZ	CT
D 2280	Dmanisi, Georgia	1.81 ± 0.03 Ma	Garcia et al., 2010	IPH	PH
D 3444	id.	id.	id.	UFR	PH
Homo erectus					
Sangiran 2	Java, Indonesia	~1.3 Ma	Matsu'ura, 2020	MH	CT
Sangiran 17	id.	id.	id.	DC	OP
Ngandong 6	id.	117–108 ka	Rizal et al., 2020	IPH	PH
Ngandong 7	id.	id.	id.	IPH	PH
Ngandong 14	id.	id.	id.	IPH	PH
Sinanthropus III	Zhoukoudian, China	0.77 ± 0.08 Ma	Shen et al., 2009	IPH	PH
Sinanthropus XI	id.	id.	id.	IPH	PH
Sinanthropus XII	id.	id.	id.	IPH	PH
Homo neanderthalensis					
Spy 1	Spy, Belgium	44.2–40.6 ka	Devièse et al., 2021	IRSNB	CT
Spy 2	id.	id.	id.	IRSNB	CT
La Chapelle aux Saints	La-Chapelle-aux-Saints, France	56 ± 4–47 ± 3 ka	Grün and Stringer, 1991	MH	CT
La Quina H5	La Quina, France	~40 ka	Frouin et al., 2017	MH	CT
Shanidar 1	Shanidar, Irak	55–45 ka	Pomeroy et al., 2020	MH	PH
Neanderthal 1	Kleine Feldhofer Grotte, Germany	~40 ka	Schmitz et al., 2002	MH	PH
Tabun C1	Tabun, Israel	122 ± 16 ka	Grün & Stringer, 2000	MH	PH
Saccopastore 1	Saccopastore, Italy	~250 ka	Marra et al., 2015	SU	PH
Monte Circeo I	Guattari cave, Monte Circeo, Italy	52 ± 12 ka	Grün and Stringer,1991	MP	CT
Gibraltar 1	Forbes' Quarry, Gibraltar	95–55 ka	Nathan, 2010	NHM	CT
La Ferrassie 1	La Ferrassie, France	54 ± 3–40 ± 2 ka	Guérin et al., 2015	MH	CT
Amud 1	Amud, Israel	70–50 ka	Valladas et al., 1999	DC	OP

(Continues)

TABLE 1 (Continued)

Specimen	Site	Chronology	Reference	Institution	3D model
Pleistocene *Homo sapiens*					
Qafzeh 6	Qafzeh, Israel	130–90 ka	Schwarcz et al., 1988	IPH	PH
Qafzeh 9	id.	id.	id.	DC	OP
Skhūl V	Skhūl, Israel	130–100 ka	Grün et al., 2005	PM	CT
Skhūl IV	id.	id.	id.	MH	PH
Omo I	Omo Kibish, Ethiopia	233 ± 22 ka	Vidal et al., 2022	FD	PH
Pataud 1	Abri Pataud, France	28–26 ka	Henry-Gambier et al., 2013	MH	CT
Předmostí III	Předmostí, Czechia	27–25 ka	Farbstein & Svoboda, 2007	MH	PH
Předmostí IV	id.	id.	id.	MH	PH
Mladec 1	Mladeč, Czechia	~31 ka	Wild et al., 2005	NHMV	CT
Pavlov 1	Dolní Věstonice, Czechia	34–30 ka	Svoboda et al., 2016	MMB	PH
Brno 3	Brno, Czechia	~24 ka	Pettitt & Trinkaus, 2000	MMB	PH
Cro-Magnon I	Les Eyzies-de-Tayac, France	28 ka	Henry-Gambier, 2002	MH	CT
NK 2	Nazlet Khater, Egypt	38 ± 6 ka	Crevecoeur et al., 2009	IC	CT
Hofmeyr 1	Hofmeyr, South Africa	36.2 ± 3.3 ka	Grine et al., 2007	ELM	PH
Holocene *Homo sapiens*					
AfE1 (AF.23.0.109)	Tanzania	19th–20th c.	M	DC	CT
AfE2 (AF.23.0.112)	Tanzania	19th–20th c.	F	DC	CT
AfC1 (AfC-4973)	Angola	19th–20th c.	M (?)	MH	PH
AfC2 (AfC-9642)	Gabon	19th–20th c.	F (?)	MH	PH
AfS1 (Kh-1739)	South Africa	19th–20th c.	M	MH	PH
AfS2 (Kh-20,323)	South Africa	19th–20th c.	M	DC	PH
AfS3 (Kh-3436)	South Africa	19th–20th c.	F	MH	PH
AfW1 (AfW-9538)	Guinea	19th–20th c.	F	MH	PH
AfW2 (AfW-9543)	Guinea	19th–20th c.	M	MH	PH
AfN1 (AfN-18,451)	Morocco	19th–20th c.	M	MH	PH
AfN2 (AfN-18,464)	Morocco	19th–20th c.	F (?)	MH	PH
Eu1 (Eu.26.00.1)	Germany	19th–20th c.	F	DC	CT
Eu2 (Eu.26.00.2)	Germany	19th–20th c.	M	DC	CT
Eu3 (Eu-12,158)	Greece	19th–20th c.	F	MH	PH
Eu4 (Eu-33,102)	Greece	19th–20th c.	M	MH	PH

Note: Original specimens are in bold.

Abbreviations: CT, Computed tomography; DC, Duckworth Laboratory of the University of Cambridge (Cambridge, United-Kingdom); ELM, East London Museum (East London, South Africa); FD, Laboratoire départemental de préhistoire du Lazaret (Fort de la Drette, France); GPUT, Geological and Palaeontological Institute of the University of Thessaloniki (Thessaloniki, Greece); IMCT, Iziko Museum of Cape Town (Cape Town, Soouth Africa); IPH, Institut de Paléontologie humaine (Paris, France); IRSNB, Institut Royal des Sciences Naturelles de Belgique (Brussels, Belgium); MH, Musée de l'Homme (Paris, France); MMB, Moravian Museum (Brno, Czech Republic); MP, Museo Pigorini (Rome, Italy); NHM, Natural History Museum (London, United-Kingdom); NHMV, Natural History Museum of Vienna (Vienna, Austria); NME, National Museum of Ethiopia (Addis-Ababa, Ethiopia); NMK, National Museums of Kenya (Nairobi, Kenya); OP, 3D scanner; PH, Photogrammetry; SU, Sapienza Università (Rome, Italy); TAZ, National Museum of Tanzania (Dar es Salaam, Tanzania).

margin (Katz & Friess, 2014; Slizewski et al., 2010) and they can be combined in a single study (Waltenberger et al., 2021).

Variation in the morphology of the human calvarium is mainly explained by neutral evolution, i.e., mutations and genetic drift (e.g., Smith, 2009; von Cramon-Taubadel, 2009). On the contrary, it has been suggested that the morphology of the upper face and the mandible were also influenced by climatic (Zaidi et al., 2017) and dietary factors (Katz et al., 2017). The extent of this influence on the face is debated (Katz et al., 2017; von Cramon-Taubadel, 2009) and it now appears likely that phenotypic variation due to diet could be dwarfed by neutral evolutionary processes (Katz et al., 2017; Mounier et al., 2018). We nevertheless chose to focus on the calvarium as it is less influenced by external factors and better reflects the evolutionary history of individuals.

2.1 | 3D geometric morphometrics

We used a set of 636 landmarks (see Figures S1 and SI2) distributed on the calvarium of each specimen of our sample, using the Landmark IDAV software (version 3.0.0.7). The semi-landmarks patches were placed following cranial sutures (i.e., bregma-lambda, lambda-asterion) and craniometric points (Bookstein, 1991) (i.e., glabella-frontomalare orbitale, frontomalare orbitale-most anteroinferior point of the temporal (MAIT), MAIT-porion, porion-asterion). Five patches of semi-landmarks were placed on the neurocranium: 4 patches of 144 semilandmarks were placed on both sides of the frontal bone and each of the parietal and temporal bones, following a line from the glabella to the lambda, and 1 patch of 64 semilandmarks was placed on the occipital bone.

Missing landmarks were estimated by mirroring and by Thin Plate Spline (TPS) interpolation using the preserved landmarks (Bookstein, 1989) for bilaterally missing landmarks (Table S2). TPS estimation was run separately for each of the groups of the comparative and study samples. This approach was applied to 45 specimens to estimate less than 3.4% of the landmarks (after mirroring, 12 specimens only presented more than 5% of missing landmarks, see Table S1). In cases of the absence of supraorbital structure, that is, for Saccopastore 1 and KNM-ES11693, missing parts were reconstructed prior to data collection using the morphological information given by the preserved surrounding areas (Harvati & Hublin, 2012). Only the glabella, the nasion, and the symmetrical semi-landmarks located on the medial point of each supraorbital arch were kept to guide the TPS reconstructions. To test for the accuracy of the TPS reconstruction of the supraorbital region following our protocol, we eliminated, on the best-preserved calvaria of our study sample, the landmarks located on this structure, and computed PCAs with the TPS-reconstructed specimens. The results show our protocol is effective, as TPS reconstructions have a very weak influence on the overall shape of the models (Figures S7–S12, Tables S4–S9). In addition, the hemi-calvaria from Narmada were reconstructed using mirroring prior to data collection.

We performed a Generalized Procrustes Analysis (GPA) (Gower, 1975; Rohlf & Slice, 1990) on the coordinates of the 3D landmarks, which removes scale, position, and orientation for each specimen in order to focus the analysis on the shape component (i.e., Procrustes shape coordinates) only. To correct for bilateral asymmetry, we used symmetrized landmark configuration of each specimen for subsequent analyses (Klingenberg, 2002). We ran a PCA on the Procrustes shape coordinates to highlight variations in the data in a reduced number of dimensions. We then modeled the shape of the calvarium for the extreme of PC1 and PC2 variation and we used these 3D warped models to visualize the main trend of morphological variation of our sample. We tested for the effect of allometry on shape (Mitteroecker, 2020), using a linear regression of the centroid size on the shape data represented by the Principal Components (PCs) coordinates. It is significant on several PCs (Table S4 and Figures S2–-S6). The influence of size on shape is a biological phenomenon that may have an impact on the study of phenetic relationships between hominin populations (Joganic & Heuzé, 2019; Maddux & Franciscus, 2009). We therefore chose to run all subsequent analyses both with the raw data (i.e., the shape data after GPA and PCA) and with the corrected data (residuals from the linear regression of the shape data on centroid size after GPA and PCA).

2.2 | Statistical analysis

We computed Multinomial Principal Component Logistic Regression (MLR) models (Moghimbeygi & Nodehi, 2022), in order to estimate the morphological affinities of the specimens of our study group with the groups of the comparative sample. As a multinomial logistic regression, MLR is used to classify several possible outcomes, that is, the different groups of our comparative sample, using predictor variables, that is, the PC scores and the residuals from the linear regression of the PC scores on the natural logarithm of the centroid size of the specimens. The models were computed using the comparative sample only and the fossils from our study sample were added to the analysis a posteriori in order to obtain their relative affinities to the comparative sample groups. We ran three different models using respectively 2, 3, and 5 PCs as variables for both raw and corrected data. Efficiency of the models was estimated using the Akaike Information Criterion (AIC) (Akaike, 1987) along with the classification accuracy of the comparative groups. We notice that increasing the number of PCs used for the models increases the accuracy of the predictions (Table 3). However, the Akaike information criterion (AIC) shows that the quality of the model is better when a small number of input variables is used (Table 2). We consequently decided to use a maximum of 5 PCs for our models GPA and PCA were performed with R (version 1.2.5033) using the Morpho package (Schlager, 2017; version 2.8), and the MLR models using the package nnet (Venables & Ripley, 2002; version 7.3–12).

3 | RESULTS

3.1 | Principal component analysis

The two first principal components (PCs) of the PCA on raw data represent 58.32% of the total variance, that is, 49.04% for PC1 and 9.28% for PC2 (Figure 1, Table S1).

Towards the positive values of the PC1 axis and in *norma lateralis*, the shape variation is mainly associated with an anterosuperior extension of the calvarium, as observed in *H. sapiens* specimens (Table S2). In the anterior part of the cranium, the supraorbital structure is gracile. In *norma occipitalis*, the parietal bones are slightly diverging superiorly and the euryon is positioned in the superior part of the parietals. In the posterior part of the cranium, the occipital squama and the nuchal plane are rounded. The overall shape of the calvarium is globular. The negative values of the PC1 correspond to a general flattening of the cranial vault at the level of the bregma. The calvarium is stretched anteroposteriorly with a strong forward projection of the supraorbital structure. In *norma occipitalis*, the parietals are converging superiorly

TABLE 2 Model summaries of fitting the MLR to raw and corrected data for the first 2, 3, and 5 PCs, showing the values of AIC, residual deviance, CoxSnell and Nagelkerke pseudo-R^2, and Hosmer-Lemeshow test.

			Pseudo-R^2		Hosmer–Lemeshow test	
Model	AIC	Residual deviance	CoxSnell	Nagelkerke	χ^2	*p*-value
Raw data 2 PCs	28.07	4.07	0.91	0.95	8.03	1.00
Corr. data 2 PCs	27.65	3.65	0.92	0.96	4.36	1.00
Raw data 3 PCs	71.16	39.16	0.90	0.95	7.95	1.00
Corr. data 3 PCs	35.06	3.05	0.93	0.96	3.14	1.00
Raw data 5 PCs	75.12	27.11	0.92	0.97	3.07	1.00
Corr. data 5 PCs	49.80	1.80	0.94	0.98	2.45	1.00

TABLE 3 Percentage of correct prediction of each group of the comparative sample using MLR for the first 2, 3, and 5 PCs both on raw and corrected data.

Accuracy	*H. ergaster*	*H. erectus*	*H. neand.*	Pleist. *H. sap.*	Hol. *H. sap.*	Total accuracy
Raw data 2 PCs	67.3%	66.4%	96.1%	70.7%	67.0%	73.5%
Corr. data 2 PCs	74.6%	71.6%	86.3%	66.4%	71.3%	74.0%
Raw data 3 PCs	59.3%	73.9%	97.9%	69.3%	71.4%	74.4%
Corr. data 3 PCs	79.4%	78.3%	96.3%	71.0%	72.9%	79.6%
Raw data 5 PCs	93.6%	94.4%	98.4%	70.1%	71.9%	85.7%
Corr. data 5 PCs	95.6%	94.3%	96.4%	75.2%	76.7%	87.6%

and the maximum of the calvarium width (euryon) is located in a low position, at the level of the *crista supramastoidea* on the temporal. In *norma lateralis*, the occipital squama is short and forms a sharp angle with the nuchal plane.

Towards the positive values of PC2, we observe in *norma occipitalis* the characteristic *H. neanderthalensis* "forme en bombe" of the calvarium, which presents a rounded profile while the euryon is located at mid-height of the calvarium. In the posterior part of the calvarium, there is a pinch at the level of the lambdoid suture associated with an occipital bun. Towards the negative values of PC2, the calvarium presents in its posterior part a more globular morphology with a more regular curvature of the two planes of the occipital. The calvarium features a receding frontal bone with a pronounced post-orbital constriction in *norma lateralis*.

The morphospace displays three main clusters, grouping respectively *H. erectus*, which overlap with *H. ergaster*, *H. neanderthalensis*, and Pleistocene and Holocene *H. sapiens*. The Middle Pleistocene hominins (MPH) present the largest distribution in the morphospace. In more detail, PC1 separates each of the five comparative sample groups albeit some overlapping, between *H. ergaster* and *H. erectus* and, predictably, between both *H. sapiens* groups. Regarding the study sample, three African specimens dated from the LMP, Irhoud 2, Omo II, and KNM-ES 11693 are positioned between *H. neanderthalensis* and *H. sapiens*. KNM-ES 11693 is close to the Levantine specimen Skhūl IV. The rest of the MPH is scattered towards the negative values of PC1 and mainly overlaps with *H. neanderthalensis* except Ceprano, which overlaps with the groups of *H. ergaster* and *H. erectus*. On average, the African MPH presents more positive values than the Eurasian MPH specimens except Kabwe 1, which seems to share strong affinities with the groups of *H. ergaster* and *H. erectus*. Holocene *H. sapiens* present more extreme positive values than Pleistocene *H. sapiens*, which is probably driven by a more derived morphology of the cranial vault which appears higher and more globular. The MPH shows a significant dispersion along this axis, while the *H. neanderthalensis* is the most cohesive group of the sample. The second PC separates *H. ergaster* and most of *H. erectus* from *H. neanderthalensis*, the latter group being located exclusively on the upper side of the morphospace.

The MPH group shows a wide dispersion in the morphospace. Several fossils plot within *H. neanderthalensis* points' cloud, including Irhoud 1, Irhoud 2, Ndutu, Jinniushan, Petralona and SH5. Kabwe 1 appears in an outlier position when compared with the rest of the African specimens, as it is closer to the *H. ergaster* and *H. erectus* distributions. The other African MPH is located closer to the Pleistocene *H. sapiens*. LH 18 and Saldanha are placed in a low position between the *H. ergaster* and the Pleistocene *H. sapiens*, while KNM-ES 11693 and, to a lesser extent, Omo II, are closer to the oldest *H. sapiens* of the sample. Among the Eurasian MPH, Ceprano occupies a very off-centred position compared to the mean configuration of the MPH. The distribution of the specimens from continental Asia is very large in the morphospace. Finally, Narmada is positioned closer to the oldest *H. sapiens* fossils, along with some African MP specimens.

Figure 2 displays the morphospace based on the residuals of the linear regression of shape on size. On PC1, it is slightly different from Figure 1 with only two main clusters: the *H. sapiens* specimens showing positive values and the rest of the sample showing negative. The specimens with a centroid size in the average of the sample are less

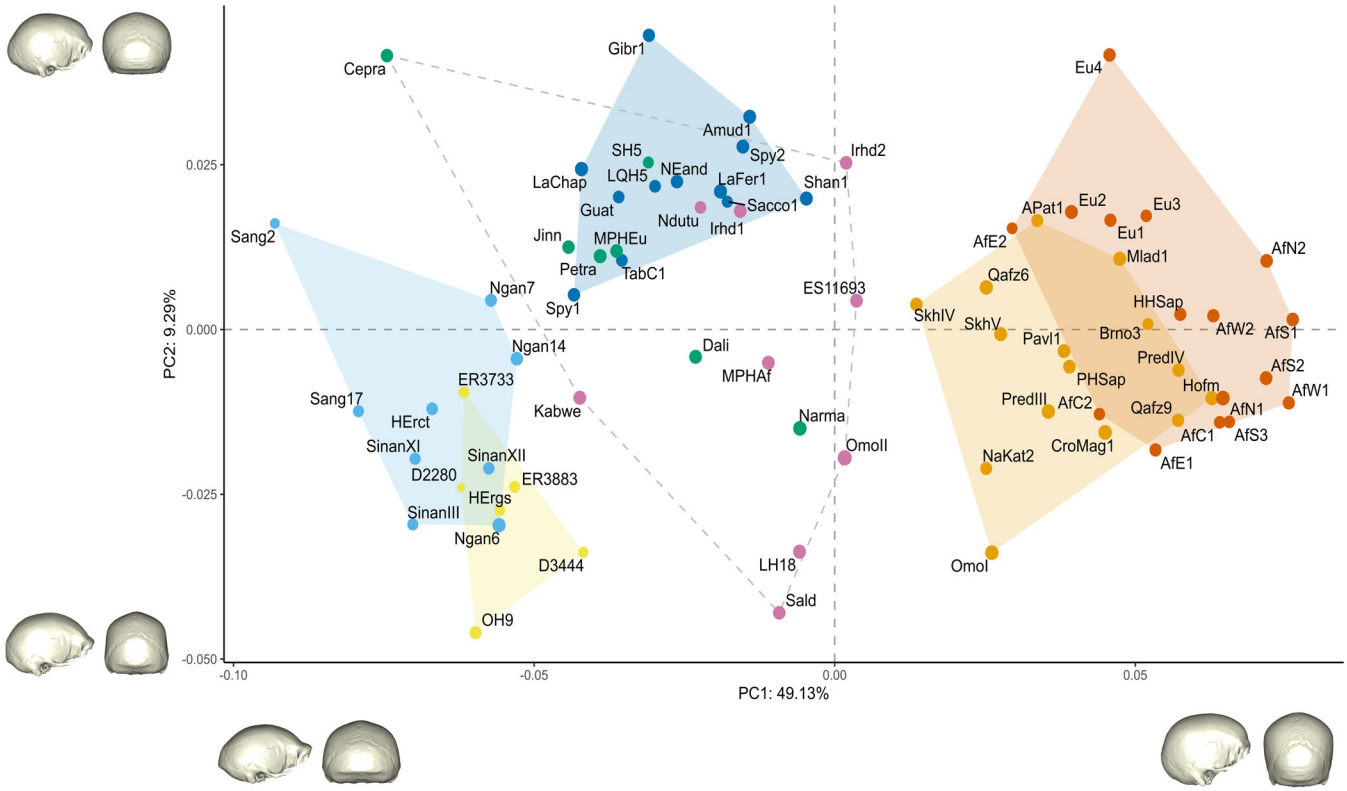

FIGURE 1 Morphospace of the first two Principal Components (PC1 and PC2) of the calvarium shape. The 3D warped models represent the shape of the calvarium for the extreme values of each PC in *norma lateralis* and *norma occipitalis*. The mean shape of each group is represented by a point: HErgs for *H. ergaster*, HErct for *H. erectus*, NEand for *H. neanderthalensis*, MPHEu for Eurasian Middle Pleistocene hominins, MPHAf for African Middle Pleistocene hominins, PHSap for Pleistocene *H. sapiens*, and HHSap for Holocene *H. sapiens*. The size of the points is proportional with the centroid size of each specimen.

sensitive to the removal of allometry. Smaller specimens shift towards higher values of the first PC while the larger ones shift towards lower values. The Pleistocene *H. sapiens* exhibit nevertheless a larger shape variation than Holocene *H. sapiens*, with the older specimens positioned closer to the fossil taxa.

All MPH groups broadly with the non-*H. sapiens* fossils at the negative end of PC 1, but vary in their affinities with *H. erectus* / *H. ergaster* and *H. neanderthalensis*. The Eurasian specimens Jinniushan and SH5 and the African fossils Irhoud 1 and Ndutu group with *H. neanderthalensis* variation, while Irhoud 2 is located close to Saccopastore 1, an early *H. neanderthalensis*. Petralona is positioned in the vicinity of the *H. erectus* Sangiran 2 and Ngandong 7 and the *H. neanderthalensis* Spy 1. Omo II and LH 18 are grouped with the *H. ergaster* of the sample and Kabwe 1 with the *H. erectus*. Compared to the other MPH, the South African specimen Saldanha scores lower along PC2. KNM-ES11693 is the closest MPH to the *H. sapiens*. At last, Dali is located, as in the PCA on raw data, between *H. ergaster* and *H. erectus* and *H. neanderthalensis*.

3.2 | Phenetic affinities

We carried out MLR models to assess the phenetic affinities of the MPH with the different groups of our study. We used the scores of the first 2, 3, and 5 PCs (i.e., raw shape data; representing respectively 58.43%, 64.43%, and 74.44% of the total variance, see Table S2) as well as the residuals of the linear regression of the centroid size of the specimens on these PCs (i.e., corrected data) as inputs for our models.

The Hosmer-Lemeshow test assesses the models' goodness of fit. The model correctly fits the data if the test statistic is not significant. Here, the Hosmer-Lemeshow statistics are not significant for every data set, meaning that all the models appropriately fit the data at the 0.05 level. The AIC shows that the models using corrected data are of better quality than those using raw data (Table 2). The models using the residuals are slightly better classifiers for the *H. ergaster*, *H. erectus*, and *H. sapiens* groups (Table 3, Tables S10–S15).

The percentage of affinities of each MPH with the groups of the comparative sample is relatively stable in the different models (Table 4 and Table 5). Most of the African specimens are classified in the *H. ergaster*, *H. erectus*, and *H. sapiens* groups while the Eurasian specimens are mostly classified in the groups of *H. ergaster*, *H. erectus*, and *H. neanderthalensis*. Several specimens are however distinguishable from this general pattern. Narmada is classified among *H. sapiens* in the models using the raw shape data but among *H. ergaster* and *H. erectus* in the models using the corrected data. Dali is classified in several groups, though proportionally more among *H. neanderthalensis* and *H. ergaster*. Ndutu differs from the other African specimens as it is

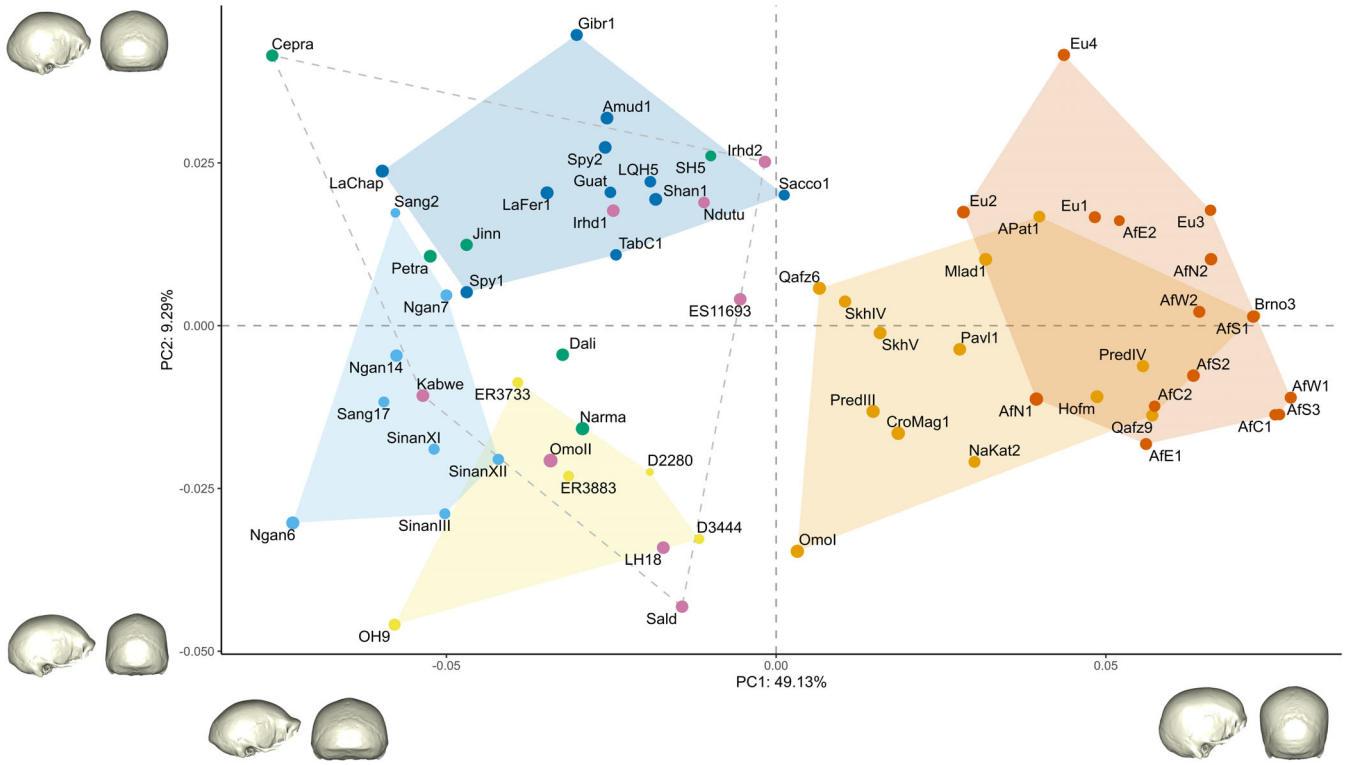

FIGURE 2 Morphospace of PC1 and PC2 of the calvarium shape based on the residuals after removing allometry. The 3D warped models represent the shape of the calvarium for the extreme values of each PC in *norma lateralis* and *norma occipitalis*.

classified among *H. neanderthalensis* in several models. Compared to the other African specimens, Kabwe 1 displays a peculiar profile, as it shares important affinities with *H. erectus* in the models using corrected data. At last, the specimens from Jebel Irhoud, as well as the Eurasian specimen SH5 and Ceprano, are classified almost exclusively among the *H. neanderthalensis* by every model.

4 | DISCUSSION

The fossil record of the MP is very scarce and the majority of the available specimens are fragmentary. Our study sample focuses on the best-preserved calvaria dating from approximately 600 ka to 150 ka in order to limit as much as possible reconstructions and estimations of missing parts. However, the scarcity of the available fossil record from this time period constitutes an important limitation to our study. The discovery of new fossil specimens from this time period along with the use and development of innovative methodological approaches, are therefore of paramount importance to help further our understanding of human evolutionary history during the MP.

Our main results highlight the important morphological variation within the analyzed MPH group. Several morphological patterns are discernible, suggesting that these fossils might represent different populations and/or species. While our results suggest overall morphological differences between African and Eurasian MPH, it appears difficult to divide them into two geographic groups. As a general trend, African fossils tend to share more affinities with *H. ergaster* and *H. sapiens* and the Eurasian specimens with *H. neanderthalensis* (Figures 3 and 4). Among these fossils, only SH5 is included in the range of variation of the *H. neanderthalensis* group in both size-corrected and raw PCA analyses, which supports its attribution to this taxon. The other specimens from Africa are out of the morphological variation of *H. sapiens*, and those from Eurasia, are out of the variation of *H. neanderthalensis*. It is therefore difficult to validate phenetically their attribution to any of these taxa. These affinities could be interpreted as an evolutionary trend towards *H. neanderthalensis* and possibly "Denisovans" in Eurasia and towards *H. sapiens* in Africa. However, some specimens do not follow this general pattern at the continental level. This would imply that lineages with different ancestries lived contemporaneously or that these different populations evolved from a common ancestor but had separate evolutionary histories. Therefore, we cannot validate the hypothesis that only two distinct lineages lived in Africa and Eurasia during the MP. Consequently, the affinities of the MPH are not entirely congruent with geography, which suggests that hypothesis 2 is valid. It is important to note that the MPH specimens included in this study, with the exception of Saldanha (Table 1), are broadly dated to the mid to late MP, a period postdating the supposed genetic last common ancestor (LCA) of *H. neanderthalensis* and *H. sapiens*, which might have lived about 700–600 ka in Africa (Meyer et al., 2016; Mounier & Mirazón Lahr, 2016; Schlebusch et al., 2017). While more recent fossils tend to share more affinities with *H. neanderthalensis* in Eurasia

TABLE 4 Percentage of classification of each MPH of the study in the different groups of the comparative sample by the MLR models using raw data for 2, 3, and 5 PCs.

Raw data 2 PCs	*H. ergaster*	*H. erectus*	*H. neand.*	Pleist. *H. sap.*	Hol. *H. sap.*	Raw data 3 PCs	*H. ergaster*	*H. erectus*	*H. neand.*	Pleist. *H. sap.*	Hol. *H. sap.*
Irhoud1	0.5%	0.0%	**98.8%**	0.6%	0.0%	Irhoud1	0.2%	0.0%	**99.6%**	0.1%	0.0%
Irhoud2	0.0%	0.0%	**97.6%**	2.2%	0.1%	Irhoud2	0.0%	0.0%	**99.9%**	0.1%	0.0%
Kabwe1	**82.5%**	5.2%	11.7%	0.6%	0.0%	Kabwe1	**52.4%**	14.3%	32.7%	0.5%	0.0%
ES11693	0.6%	0.0%	21.5%	**76.7%**	1.2%	ES11693	1.9%	0.0%	24.9%	**72.5%**	0.6%
Saldanha	4.1%	0.0%	0.0%	**95.9%**	0.0%	Saldanha	5.0%	0.0%	0.0%	**95.0%**	0.0%
Ndutu	0.7%	0.0%	**99.1%**	0.2%	0.0%	Ndutu	34.3%	2.4%	**58.8%**	4.4%	0.0%
LH18	2.5%	0.0%	0.0%	**97.4%**	0.0%	LH18	4.1%	0.0%	0.0%	**95.9%**	0.0%
OmoII	0.7%	0.0%	0.2%	**98.9%**	0.2%	OmoII	1.9%	0.0%	0.0%	**98.0%**	0.1%
Petralona	6.8%	1.3%	**91.9%**	0.1%	0.0%	Petralona	5.4%	4.4%	**90.1%**	0.0%	0.0%
SH5	0.3%	0.0%	**99.7%**	0.0%	0.0%	SH5	1.4%	0.9%	**97.7%**	0.0%	0.0%
Ceprano	0.0%	**78.5%**	21.5%	0.0%	0.0%	Ceprano	0.0%	**77.2%**	22.8%	0.0%	0.0%
Jinn.	6.6%	4.1%	**89.3%**	0.0%	0.0%	Jinn.	1.9%	4.3%	**93.9%**	0.0%	0.0%
Narmada	3.8%	0.0%	1.5%	**94.5%**	0.1%	Narmada	8.5%	0.0%	0.1%	**91.3%**	0.1%
Dali	35.3%	0.1%	**50.0%**	14.6%	0.0%	Dali	25.1%	0.5%	**66.4%**	8.0%	0.0%

Raw data 5 PCs	*H. ergaster*	*H. erectus*	*H. neand.*	Pleist. *H. sap.*	Hol. *H. sap.*
Irhoud1	0.1%	0.0%	**99.7%**	0.2%	0.0%
Irhoud2	0.0%	0.0%	**99.5%**	0.5%	0.0%
Kabwe1	**51.9%**	23.8%	24.0%	0.3%	0.0%
ES11693	0.1%	0.0%	2.0%	**97.7%**	0.2%
Saldanha	1.2%	0.0%	0.0%	**98.8%**	0.0%
Ndutu	28.9%	0.1%	**63.3%**	7.7%	0.0%
LH18	0.8%	0.0%	0.0%	**99.1%**	0.0%
OmoII	0.1%	0.0%	0.0%	**99.7%**	0.1%
Petralona	3.0%	0.1%	**96.9%**	0.0%	0.0%
SH5	0.3%	0.0%	**99.7%**	0.0%	0.0%
Ceprano	0.0%	**82.9%**	17.1%	0.0%	0.0%
Jinn.	1.6%	13.4%	**84.9%**	0.0%	0.0%
Narmada	2.1%	0.2%	0.6%	**97.1%**	0.1%
Dali	22.0%	0.1%	**59.8%**	18.2%	0.0%

Note: Percentage of classification exceeding 50% are given in bold.

and *H. sapiens* in Africa, several penecontemporaneous specimens present affinities with more basal taxa, meaning that the affinities of the MP fossils are not entirely congruent with chronology, as postulated in hypothesis 3.

The African specimens KNM-ES 11693, Saldanha, LH 18, and Omo II share strong affinities with Pleistocene *H. sapiens*, and with *H. ergaster* and *H. erectus* (Figures 3 and 4, Table 4 and Table 5). KNM-ES 11693 is the specimen that shares the most affinities with *H. sapiens* in both the models with raw and corrected data. However, KNM-ES 11693 presents a pathological alteration of the calvarium with an important increase in the bone thickness, notably a broadening symmetrical to the sagittal suture (Bräuer et al., 2003). Such a condition could have possibly contributed to the increase in the general globular shape of the cranial vault and facilitated the classification of the specimen as *H. sapiens*. However, according to the results displayed in Table 1 by Bräuer et al. (2003), the pathologically thickened cranial vault of KNM-ES 11693 deviates from the expected variation from ~3 to ~6 mm (depending on the reference group) and it would seem unlikely that this could have had a strong impact on the global shape of the calvarium. It is interesting to note that the results from the models using corrected data increase the likelihood of Saldanha, LH 18 and Omo II to be classified as *H. erectus* (see Figures 3 and 4). It appears therefore that the shape of the calvarium of these specimens, when taking off the influence of size, is more reminiscent of *H. erectus* than of *H. sapiens*. These fossils exhibit morphological features found in *H. erectus*—a strong angulation of the occipital bone and a

TABLE 5 Percentage of classification of each MPH of the study in the different groups of the comparative sample by the MLR models using corrected data for 2, 3, and 5 PCs.

Corr. Data 2 PCs	*H. ergaster*	*H. erectus*	*H. neand.*	Pleist. *H. sap.*	Hol. *H. sap.*	Corr. Data 3 PCs	*H. ergaster*	*H. erectus*	*H. neand.*	Pleist. *H. sap.*	Hol. *H. sap.*
Irhoud1	2.6%	0.9%	**96.4%**	0.0%	0.0%	Irhoud1	0.2%	0.0%	**99.8%**	0.0%	0.0%
Irhoud2	1.2%	0.0%	**97.5%**	1.2%	0.1%	Irhoud2	0.0%	0.0%	**100.0%**	0.0%	0.0%
Kabwe1	10.5%	**86.5%**	3.1%	0.0%	0.0%	Kabwe1	9.5%	**85.4%**	5.1%	0.0%	0.0%
ES11693	35.0%	0.1%	44.9%	19.4%	0.6%	ES11693	36.2%	0.0%	46.7%	16.8%	0.3%
Saldanha	**88.2%**	0.0%	0.0%	11.7%	0.0%	Saldanha	**93.0%**	0.0%	0.0%	7.0%	0.0%
Ndutu	3.1%	0.1%	**96.2%**	0.5%	0.0%	Ndutu	35.7%	0.5%	**61.6%**	2.0%	0.1%
LH18	**93.0%**	0.1%	0.1%	6.8%	0.0%	LH18	**97.6%**	0.0%	0.0%	2.3%	0.0%
OmoII	**89.6%**	8.3%	1.9%	0.2%	0.0%	OmoII	**87.1%**	12.9%	0.0%	0.0%	0.0%
Petralona	1.6%	**63.4%**	35.0%	0.0%	0.0%	Petralona	0.6%	**70.6%**	28.9%	0.0%	0.0%
SH5	0.8%	0.0%	**99.0%**	0.2%	0.0%	SH5	0.3%	0.0%	**99.7%**	0.0%	0.0%
Ceprano	0.0%	**66.4%**	33.6%	0.0%	0.0%	Ceprano	0.0%	**95.6%**	4.4%	0.0%	0.0%
Jinn.	2.3%	37.2%	**60.5%**	0.0%	0.0%	Jinn.	0.3%	5.4%	**94.3%**	0.0%	0.0%
Narmada	**90.1%**	5.0%	4.4%	0.6%	0.0%	Narmada	**95.6%**	4.3%	0.0%	0.0%	0.0%
Dali	**56.0%**	13.9%	29.9%	0.2%	0.0%	Dali	49.9%	2.6%	47.5%	0.0%	0.0%

Corr. Data 5 PCs	*H. ergaster*	*H. erectus*	*H. neand.*	Pleist. *H. sap.*	Hol. *H. sap.*
Irhoud1	0.9%	0.0%	**99.1%**	0.0%	0.0%
Irhoud2	0.3%	0.0%	**99.4%**	0.3%	0.0%
Kabwe1	0.3%	**99.4%**	0.3%	0.0%	0.0%
ES11693	18.6%	0.0%	0.5%	**80.9%**	0.0%
Saldanha	**94.0%**	0.0%	0.0%	6.0%	0.0%
Ndutu	**81.6%**	0.0%	1.9%	16.4%	0.0%
LH18	90.9%	0.8%	0.0%	8.3%	0.0%
OmoII	**65.3%**	34.7%	0.0%	0.0%	0.0%
Petralona	0.6%	22.6%	**76.8%**	0.0%	0.0%
SH5	2.3%	0.0%	**97.3%**	0.4%	0.0%
Ceprano	0.0%	**60.2%**	39.8%	0.0%	0.0%
Jinn.	0.5%	30.3%	**69.2%**	0.0%	0.0%
Narmada	0.3%	**99.7%**	0.0%	0.0%	0.0%
Dali	**70.3%**	8.4%	21.3%	0.0%	0.0%

Note: Percentage of classification exceeding 50% are given in bold.

protruding supraorbital suture for instance—associated with traits found in *H. sapiens*, such as a relatively higher neurocranium and a larger cranial capacity (Lieberman, 2011). The important phenetic affinities of these fossils with *H. sapiens* indicate they might represent ancestral populations to this species. This suggests that diverse populations distributed across Africa might have contributed to that of *H. sapiens* (Hublin et al., 2017; Mounier & Mirazón Lahr, 2019; Bergström et al., 2021; Andirkó et al., 2022). Following geographic and demographic fluctuations, these populations may have taken part in the origin of *H. sapiens* in different proportions (Mirazón Lahr, 2016; Mounier & Mirazón Lahr, 2019). However, to our knowledge, Saldanha, which is imprecisely dated to about 600 ka (Klein et al., 2007), have never been interpreted as an African MPH whose morphology is reminiscent of *H. sapiens* (e.g., Rightmire, 1998, 2008; Lieberman, 2011; Mounier, 2009).

Ndutu, broadly dated to 400–200 ka (Rightmire, 1983), shares affinities with several groups. Along with the specimens from Jebel Irhoud, it is the only African specimen to share important affinities with *H. neanderthalensis* in some of the models. This specimen has however been subjected to an important reconstruction (Clark, 1976), notably on the frontal and the parietal bones. The rather gracile aspect of Ndutu's morphology compared to the other African MPH might also be due to sexual dimorphism (Harvati & Reyes-Centeno, 2022).

The specimen from Zambi', Kabwe 1, is never classified in the group of the Pleistocene *H. sapiens*. In the models using the residuals, it is mostly classified among *H. ergaster*. Such a result highlights the robust aspect of its calvarium compared to other African MPH specimens. Initially placed among the first African specimens to feature a morphology clearly distinguishable from *H. erectus* along with Saldanha (Rightmire, 2001), it has been recently dated to about 299 ka

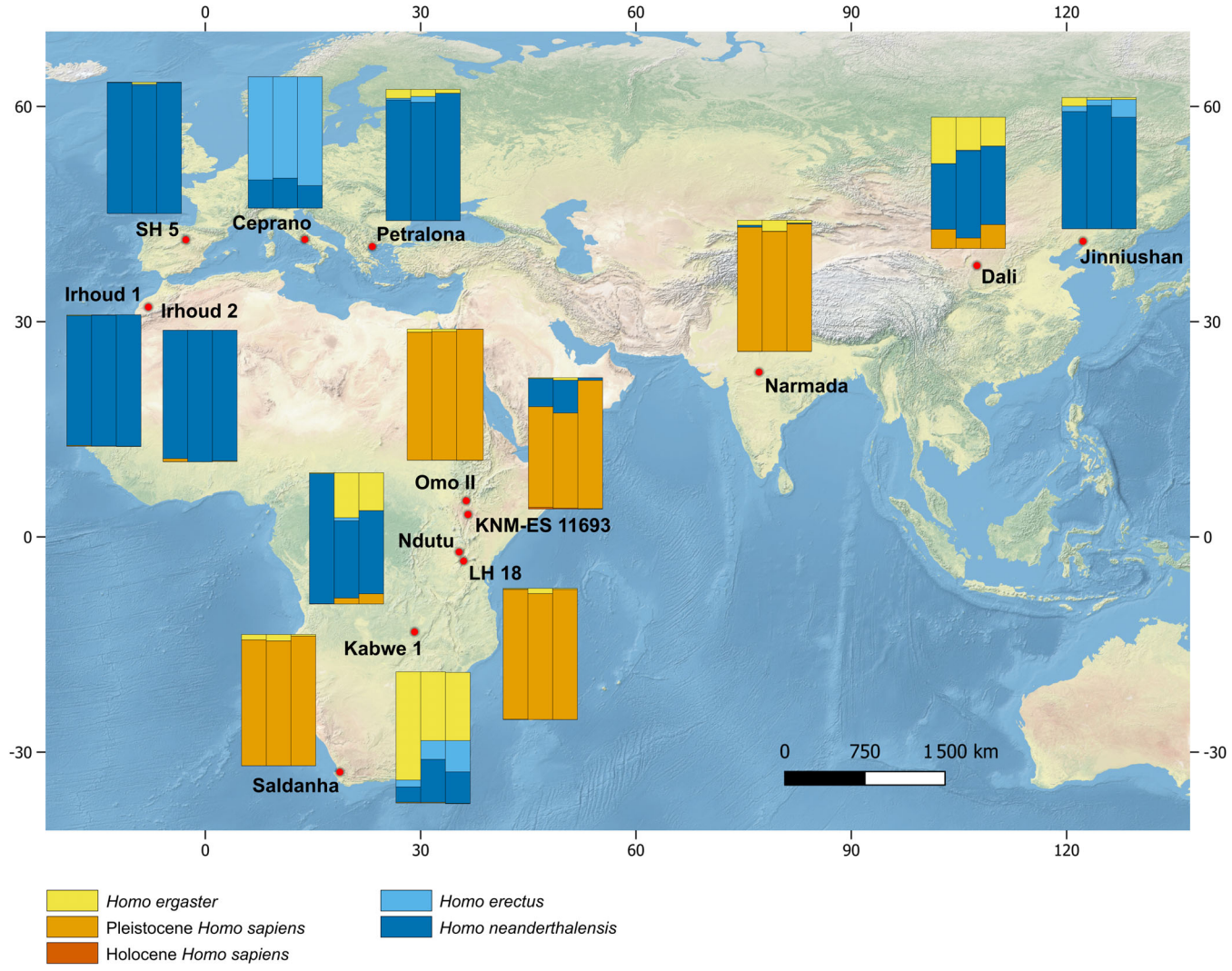

FIGURE 3 Map of the sites where the MPH fossils of the study sample have been recovered. Bar plots represent the proportion of classification of each MPH in the different groups of the comparative sample (see Table 4) using raw data for the first 2, 3, and 5 PCs (from left to right).

(Grün et al., 2020). Kabwe 1 is thus penecontemporaneous to other East African fossils, which exhibit a morphology much closer to *H. sapiens*. Stringer (1983, 2012), Rightmire (2015, 2017), and Mounier et al. (2009, 2011) have shown the strong morphological similarities of Kabwe 1 with the specimen from Greece, Petralona. Both fossils share important affinities with the *H. ergaster*. It seems therefore possible that these specimens come from populations that are phylogenetically close, and that repeated contacts happened between African and Eurasian populations. This hypothesis is corroborated by a palaeoenvironmental study carried out by Bailey and colleagues (2019) which showed that periods of low sea level (i.e., corresponding to transitions between glacial and interglacial periods) were accompanied by better climatic conditions during the last 400 ka in the Mediterranean basin, which may have favored the mobility of hominins. Recent discoveries of sites with Acheulean lithic industry in the Greek archipelago, also seem to show the existence of a migration route following the coasts of southern Europe during this period (Tourloukis & Harvati, 2018; Tsakanikou et al., 2020; Konidaris et al., 2023).

The Eurasian specimens Ceprano, Petralona, SH5, and Jinniushan share important affinities with *H. neanderthalensis*. Ceprano is mainly classified as *H. neanderthalensis*. Its peculiar morphology, which retains characteristics observable in *H. erectus* associated with features displayed by other MPH, has been shown by several studies (Mounier et al., 2011; Manzi, 2016; Di Vincenzo et al., 2017). If we consider the dating of Ceprano between 430 and 385 ka (Manzi et al., 2010) and its morphology, it is likely that this fossil originated from a population that came from Africa to Europe at the beginning of the Middle Pleistocene. The first occurrence of the Acheulean in Europe is documented in the South of the Italian peninsula at Notarchirico, as well as at La Noira and Moulin Quignon, in central France at around 700 ka (Moncel, Despriée, et al., 2020; Moncel et al., 2020; Antoine

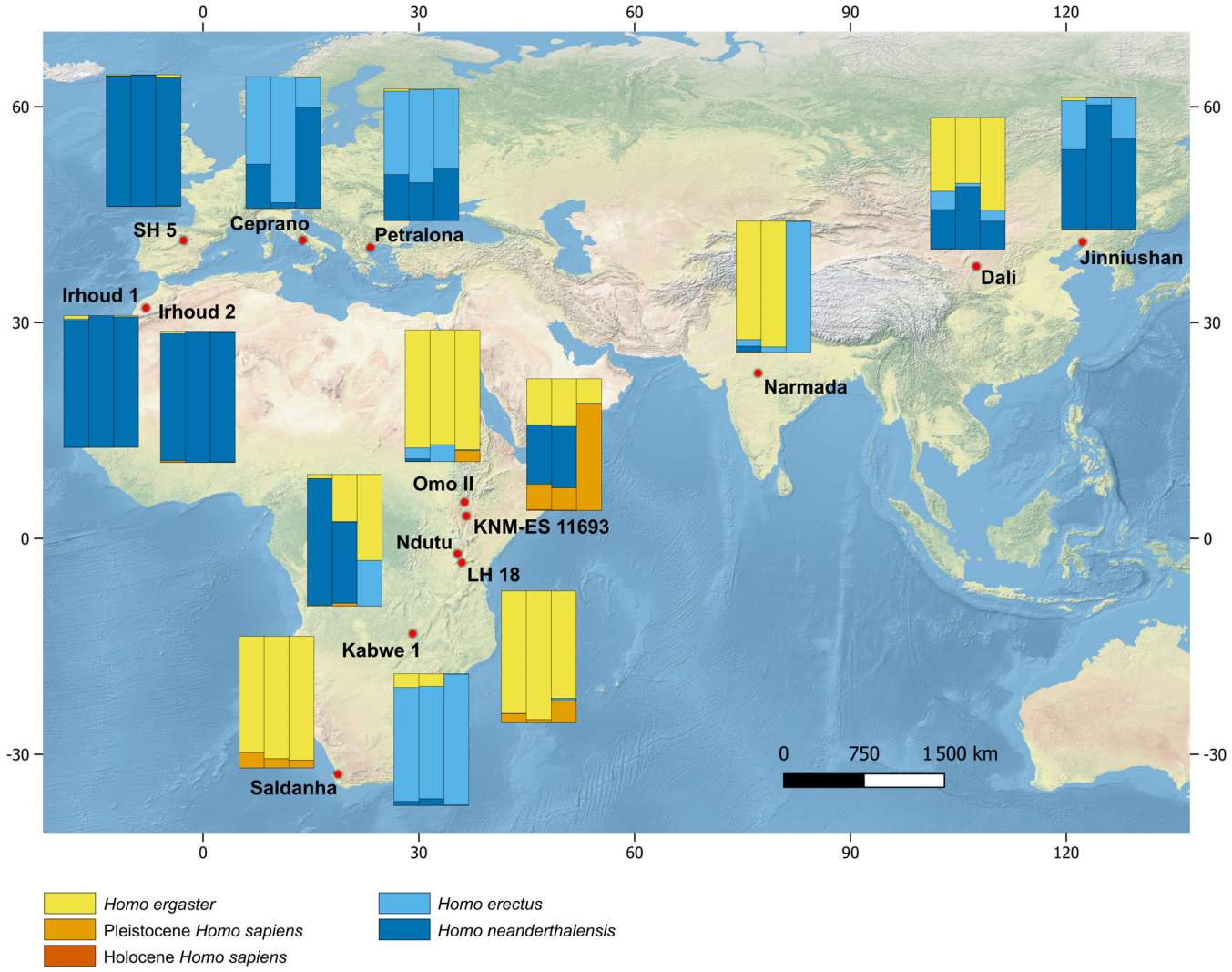

FIGURE 4 Map of the sites where the MPH fossils of the study sample have been recovered. Bar plots represent the proportion of classification of each MPH in the different groups of the comparative sample (see Table 5) using corrected data for the first 2, 3, and 5 PCs (from left to right).

et al., 2019), which is corresponds to, or slightly predates, the genetic split between *H. neanderthalensis* and *H. sapiens*. Following a period of probable depopulation of Europe around 1.1 Ma: (Margari et al., 2023), the arrival of new hominin populations in Eurasia may then have been favored by the extension of grasslands to higher latitudes towards the end of the Middle Pleistocene Transition (i.e., from 1.25 Ma to ca. 700 ka; Dean et al., 2015) and the subsequent opening of migration corridors from East Africa in particular (Abbate & Sagri, 2012; Beyin et al., 2019; Head & Gibbard, 2015). In Africa, hominin populations may have suffered a major bottleneck between approximately 930 to 810 ka, leading to a dramatic loss of genetic diversity (Hu et al., 2023). In Eurasia, some regions, such as Iberia, the Italian peninsula, and the Balkans, might have served as refugia zones during periods of climatic deterioration, favoring bottleneck effects and sometimes leading to extinctions (Dennell et al., 2011).

SH5 is exclusively classified in the group of *H. neanderthalensis*. This is consistent with several paleoanthropological (e.g., Arsuaga et al., 2014; Mounier & Caparros, 2015) and genetic studies (Meyer et al., 2016) which have shown that the fossils from the Sima de los Huesos (SH, Spain) are early representatives of *H. neanderthalensis*.

Jinniushan calvarium exhibits important affinities with the specimens from Western Europe, notably Petralona, and is often classified with *H. neanderthalensis* by the models. Dated to about 270 ka (Rosenberg et al., 2006), it is often grouped with other LMP fossils from continental China, such as Dali (Hublin, 2013; Ao et al., 2017; Wu et al., 2019; Ni, 2021; Mounier, 2011), while the shape of its calvarium was found to show affinities with *H. neanderthalensis* (Mounier, 2009; Mounier et al., 2011). The fossil from Dali, which presents affinities with several groups, stands out from the rest of the specimens from Eurasia. Its morphology, more robust than Jinniushan's, is sometimes interpreted as sexual dimorphism within the same population (Kaifu, 2017). Some researchers also explain its peculiar morphology by the existence of several populations in continental China evolving in a braided stream network of gene flow (Athreya &

Wu, 2017). Genetic studies (Meyer et al., 2014; Reich et al., 2010) and new discoveries (Chen et al., 2019; Demeter et al., 2022) have shown that a sister group of the *H. neanderthalensis* sharing the same mtDNA as the individuals from SH, often referred as the "Denisovans" (Reich et al., 2010), was living in Asia during LMP. It is therefore probable that these specimens from continental China are ancestral to this population (Di Vincenzo & Manzi, 2023). In addition, a recent phylogenetic study (Ni, 2021), suggested that Jinniushan and Dali are part of the same clade as the newly found cranium from Harbin in Northern China, and Ji and collaborators (2021) proposed that they should be integrated into a new taxon, *H. longi*. However, the attribution of the specimens described as potential "Denisovans" to this new taxon remains to be clarified.

The fossil from the Indian subcontinent Narmada is the only Eurasian specimen to be classified in the *H. sapiens* group by the models using raw data. In this regard, Narmada resembles some of the African MPH. It is however important to note that this fossil, a hemicalvarium, has been virtually reconstructed by mirroring. It exhibits a peculiar morphology with morphological features found in *H. erectus* associated with characters found in *H. sapiens* and specific traits (Kennedy, 2014), making it difficult to decipher its phylogenetic relations (Athreya, 2007; Cameron et al., 2004; Sankhyan, 2020).

Irhoud 1 and 2 are the only African specimens to be classified almost exclusively among *H. neanderthalensis* by every model. However, the shape of the Jebel Irhoud specimens' faces (i.e., Irhoud 1 and 10) has been shown to share affinities with *H. sapiens* (Hublin et al., 2017; Mounier, 2012). It has therefore been proposed that they should be placed at the root of *the H. sapiens* lineage (Hublin et al., 2017). Posth et al. (2017), in a recent genetic study, showed that the ancestral Neanderthal mtDNA was replaced by an African mtDNA between 400 and 260 ka. In addition, Petr et al. (2020) showed that gene flows from Africa also replaced the Y-chromosome DNA of Middle Pleistocene European populations between 450 and 100 ka. The Jebel Irhoud specimens, given their particularly *H. neanderthalensis*-like morphology compared to LMP African fossils (Mounier & Mirazón Lahr, 2019), their dating (i.e., about 315 ka, Richter et al., 2017) and their geographical origin, could represent a lineage of which some members would have hybridized with a European population in the Middle Pleistocene. However, this hypothesis remains difficult to confirm as the fossil record for this period is scarce and presents very few precisely dated fossils (Hublin, 2013). Moreover, the effect of hybridization on the phenotype is still poorly understood, despite increasing interest in the subject (e.g., Gunz et al., 2019; Harvati & Ackermann, 2022).

Additional taxonomical hypotheses have been made regarding the classification of the controversial MP fossils, the most recent being the introduction of a new species named, *H. bodoensis*, to accommodate some of the African MP fossils (Roksandic et al., 2022). Nevertheless, it is not clear how the change of a species' name contributes to the clarifying of the phylogenetic relationships between these fossils. The present study offers an alternative evolutionary hypothesis to the dichotomy between the classic Afro-European (i.e., *H. heidelbergensis s.l.* as a unique Afro-European species) and European (*H. heidelbergensis s.s.* or *H. neanderthalensis* in Europe and *H. rhodesiensis*/*H. bodoensis* in Africa) *H. heidelbergensis* hypotheses. Though being limited to the morphology of the calvarium, our results allow us to draw a framework for human evolution during LMP. In Africa, several populations may have existed contemporaneously at the continental level, with local morphs retaining *H. erectus*-like features and others exhibiting more derived, pre-*sapiens* morphologies, in the East and the South of the continent. Such a result is congruent with the study by Mounier and Mirazón Lahr (2019), which showed that *H. sapiens* might have originated in these regions of Africa. Phases of expansion may have led to hybridizations while the increased fragmentation could have caused local extinctions eventually resulting in the emergence of *H. sapiens*, which could constitute a speciation event. *H. sapiens* is first documented in the fossil record with Omo I (Ethiopia), dated to at least 233 ka (Vidal et al., 2022). In Eurasia, populations display a pre-*H. neanderthalensis* morphology in western Europe seems to have spread across the continent from over 400 ka with local morphological variants which could have resulted from several founder effects or hybridization with archaic populations, such as in Southern Europe or continental Asia. In this latter region, a local morph could probably be identified, with the fossils from Dali and Jinniushan, to the "Denisovans". More fossils from this part of the world would however be necessary to further those conclusions.

AUTHOR CONTRIBUTIONS

Hugo Hautavoine: Conceptualization (equal); formal analysis (equal); investigation (lead); methodology (equal); project administration (equal); visualization (lead); writing – original draft (lead). **Julie Arnaud:** Conceptualization (supporting); formal analysis (supporting); methodology (supporting); supervision (supporting); validation (supporting); writing – review and editing (supporting). **Antoine Balzeau:** Methodology (supporting); supervision (lead); validation (supporting); writing – review and editing (lead). **Aurélien Mounier:** Conceptualization (equal); formal analysis (equal); methodology (equal); project administration (equal); resources (lead); supervision (lead); validation (lead); writing – review and editing (lead).

ACKNOWLEDGMENTS

The authors would like to thank the institutions, which have provided us with the material of this study: the Musée de l'Homme and the Institut de Paléontologie humaine (Paris, France), the Laboratoire départemental de préhistoire du Lazaret (Fort de la Drette, France), the National Museums of Kenya (Nairobi, Kenya), the Duckworth Laboratory of the University of Cambridge (Cambridge, United-Kingdom), the National Museum of Ethiopia (Addis-Ababa, Ethiopia), the Museo Pigorini (Rome, Italy), the East London Museum (East London, South Africa), the Institut Royal des Sciences Naturelles de Belgique (Brussels, Belgium), the Iziko Museum of Cape Town (Cape Town, South Africa), the Natural History Museum (London, United-Kingdom), the Sapienza Università (Rome, Italy) the Geological and Palaeontological Institute of the University of Thessaloniki (Thessaloniki, Greece), the National Museum of Tanzania

(Dar es Salaam, Tanzania), the Natural History Museum of Vienna (Vienna, Austria) and the Moravian Museum (Brno, Czech Republic). The authors also thank the coordinator of the ANR project "Big Dry" (ANR-14-CE31), Pr. François Bon and collaborators Dr. Isabelle Crèvecoeur, Dr. David Pleurdeau, Dr. Joséphine Lesur and Dr. Chantal Tribolo for having given us access to the 3D model of Nazlet Khater 2.

DATA AVAILABILITY STATEMENT

The data that supports the findings of this study are available in the supplementary material of this article.

ORCID

Hugo Hautavoine https://orcid.org/0000-0002-3462-8184
Aurélien Mounier https://orcid.org/0000-0001-9713-7246

REFERENCES

Abbate, E., & Sagri, M. (2012). Early to middle Pleistocene homo dispersals from Africa to Eurasia: Geological, climatic and environmental constraints. *Quaternary International*, *17*, 3–19.

Akaike, H. (1987). Factor analysis and AIC. *Psychometrika*, *52*(3), 317–332. https://doi.org/10.1007/BF02294359

Andirkó, A., Moriano, J., Vitriolo, A., Kuhlwilm, M., Testa, G., & Boeckx, C. (2022). Temporal mapping of derived high-frequency gene variants supports the mosaic nature of the evolution of *Homo sapiens*. *Scientific Reports*, *12*(1), 9937. https://doi.org/10.1038/s41598-022-13589-0

Antoine, P., Moncel, M.-H., Voinchet, P., Locht, J.-L., Amselem, D., Hérisson, D., Hurel, A., & Bahain, J.-J. (2019). The earliest evidence of Acheulian occupation in Northwest Europe and the rediscovery of the moulin Quignon site, Somme Valley, France. *Scientific Reports*, *9*(1), 13091. https://doi.org/10.1038/s41598-019-49400-w

Ao, H., Liu, C.-R., Roberts, A. P., Zhang, P., & Xu, X. (2017). An updated age for the Xujiayao hominin from the Nihewan Basin, North China: Implications for middle Pleistocene human evolution in East Asia. *Journal of Human Evolution*, *106*, 54–65. https://doi.org/10.1016/j.jhevol.2017.01.014

Arnold, L. J., Demuro, M., Parés, J. M., Arsuaga, J. L., Aranburu, A., Bermúdez de Castro, J. M., & Carbonell, E. (2014). Luminescence dating and palaeomagnetic age constraint on hominins from Sima de los Huesos, Atapuerca, Spain. *Journal of Human Evolution*, *67*, 85–107. https://doi.org/10.1016/j.jhevol.2013.12.001

Arsuaga, J., Carretero, J., Lorenzo, C., Gracia, A., Martínez, I., Bermúdez de Castro, J.-M., & Carbonell, E. (1997). Size variation in middle Pleistocene humans. *Science (New York, N.Y.)*, *277*, 1086–1088. https://doi.org/10.1126/science.277.5329.1086

Arsuaga, J. L., Martínez, I., Arnold, L. J., Aranburu, A., Gracia-Téllez, A., Sharp, W. D., Quam, R. M., Falguères, C., Pantoja-Pérez, A., Bischoff, J., Poza-Rey, E., Parés, J. M., Carretero, J. M., Demuro, M., Lorenzo, C., Sala, N., Martinón-Torres, M., García, N., de Velasco, A. A., … Carbonell, E. (2014). Neandertal roots: Cranial and chronological evidence from Sima de los Huesos. *Science*, *344*(6190), 1358–1363. https://doi.org/10.1126/science.1253958

Athreya, S. (2007). Was *Homo heidelbergensis* in South Asia? A test using the Narmada fossil from central India. In M. D. Petraglia & B. Allchin (Eds.), *The evolution and history of human populations in South Asia: Inter-disciplinary studies in archaeology, biological anthropology, linguistics and genetics* (pp. 137–170). Springer. https://doi.org/10.1007/1-4020-5562-5_7

Athreya, S., & Wu, X. (2017). A multivariate assessment of the Dali hominin cranium from China: Morphological affinities and implications for Pleistocene evolution in East Asia. *American Journal of Physical Anthropology*, *164*(4), 679–701. https://doi.org/10.1002/ajpa.23305

Bailey, G. N., Meredith-Williams, M., Alsharekh, A., & Hausmann, N. (2019). The archaeology of pleistocene coastal environments and human dispersals in the Red Sea: Insights from the Farasan Islands. In N. M. A. Rasul & I. C. F. Stewart (Eds.), *Geological Setting, Palaeoenvironment and Archaeology of the Red Sea* (pp. 583–604). Springer International Publishing. https://doi.org/10.1007/978-3-319-99408-6_26

Bergström, A., Stringer, C., Hajdinjak, M., Scerri, E. M. L., & Skoglund, P. (2021). Origins of modern human ancestry. *Nature*, *590*(7845), 229–237. https://doi.org/10.1038/s41586-021-03244-5

Beyin, A., Hall, J., & Day, C. A. (2019). A least cost path model for hominin dispersal routes out of the east African rift region (Ethiopia) into the levant. *Journal of Archaeological Science: Reports*, *23*, 763–772. https://doi.org/10.1016/j.jasrep.2018.11.024

Bookstein, F. L. (1989). "Size and Shape": A Comment on Semantics. *Systematic Zoology*, *38*(2), 173–180. https://doi.org/10.2307/2992387

Bookstein, F. L. (1991). *Morphometric Tools for Landmark Data: Geometry and Biology*. Cambridge University Press.

Bräuer, G. (2008). The origin of modern anatomy: By speciation or intraspecific evolution? *Evolutionary Anthropology: Issues, News, and Reviews*, *17*(1), 22–37. https://doi.org/10.1002/evan.20157

Bräuer, G., Groden, C., Delling, G., Kupczik, K., Mbua, E., & Schultz, M. (2003). Pathological alterations in the archaic *Homo sapiens* cranium from Eliye Springs, Kenya. *American Journal of Physical Anthropology*, *120*(2), 200–204. https://doi.org/10.1002/ajpa.10144

Cameron, D., Patnaik, R., & Sahni, A. (2004). The phylogenetic significance of the middle Pleistocene Narmada hominin cranium from central India. *International Journal of Osteoarchaeology*, *14*(6), 419–447. https://doi.org/10.1002/oa.725

Chen, F., Welker, F., Shen, C.-C., Bailey, S. E., Bergmann, I., Davis, S., Xia, H., Wang, H., Fischer, R., Freidline, S. E., Yu, T.-L., Skinner, M. M., Stelzer, S., Dong, G., Fu, Q., Dong, G., Wang, J., Zhang, D., & Hublin, J.-J. (2019). A late middle Pleistocene Denisovan mandible from the Tibetan plateau. *Nature*, *569*(7756), 409–412. https://doi.org/10.1038/s41586-019-1139-x

Clark, R. J. (1976). New cranium of *Homo erectus* from Lake Ndutu, Tanzania. *Nature*, *262*(5568), 5568. https://doi.org/10.1038/262485a0

Crevecoeur, I., Rougier, H., Grine, F., & Froment, A. (2009). Modern human cranial diversity in the Late Pleistocene of Africa and Eurasia: Evidence from Nazlet Khater, Peştera cu Oase, and Hofmeyr. *American Journal of Physical Anthropology*, *140*(2), 347–358. https://doi.org/10.1002/ajpa.21080

Dean, W. E., Kennett, J. P., Behl, R. J., Nicholson, C., & Sorlien, C. C. (2015). Abrupt termination of marine isotope stage 16 (termination VII) at 631.5 ka in Santa Barbara Basin, California. *Paleoceanography*, *30*(10), 1373–1390. https://doi.org/10.1002/2014PA002756

DeMenocal, P. B. (2011). Climate and human evolution. *Science*, *331*(6017), 540–542. https://doi.org/10.1126/science.1190683

Demeter, F., Zanolli, C., Westaway, K. E., Joannes-Boyau, R., Duringer, P., Morley, M. W., Welker, F., Rüther, P. L., Skinner, M. M., McColl, H., Gaunitz, C., Vinner, L., Dunn, T. E., Olsen, J. V., Sikora, M., Ponche, J.-L., Suzzoni, E., Frangeul, S., Boesch, Q., … Shackelford, L. (2022). A middle Pleistocene Denisovan molar from the Annamite chain of northern Laos. *Nature Communications*, *13*(1), 1. https://doi.org/10.1038/s41467-022-29923-z

Dennell, R. W. (2008). Human migration and occupation of Eurasia. *Episodes Journal of International Geoscience*, *31*(2), 207–210. https://doi.org/10.18814/epiiugs/2008/v31i2/003

Dennell, R. W., Martinón-Torres, M., & Bermúdez de Castro, J. M. (2011). Hominin variability, climatic instability and population demography in middle Pleistocene Europe. *Quaternary Science Reviews*, *30*(11), 1511–1524. https://doi.org/10.1016/j.quascirev.2009.11.027

Devièse, T., Abrams, G., Hajdinjak, M., Pirson, S., Groote, I. D., Modica, K. D., Toussaint, M., Fischer, V., Comeskey, D., Spindler, L.,

Meyer, M., Semal, P., & Higham, T. (2021). Reevaluating the timing of Neanderthal disappearance in Northwest Europe. *Proceedings of the National Academy of Sciences*, *118*(12). https://doi.org/10.1073/pnas.2022466118

Di Vincenzo, F., Profico, A., Bernardini, F., Cerroni, V., Dreossi, D., Schlager, S., Zaio, P., Benazzi, S., Biddittu, I., Rubini, M., Tuniz, C., & Manzi, G. (2017). Digital reconstruction of the Ceprano calvarium (Italy), and implications for its interpretation. *Scientific Reports*, *7*(1), 13974. https://doi.org/10.1038/s41598-017-14437-2

Di Vincenzo, F., & Manzi, G. (2023). *Homo heidelbergensis* as the middle Pleistocene common ancestor of Denisovans, Neanderthals and modern humans. *Journal of Mediterranean Earth Sciences*, *15*. https://doi.org/10.13133/2280-6148/18074

Duesing, W., Kaboth-Bahr, S., Asrat, A., Cohen, A. S., Foerster, V., Lamb, H. F., Schaebitz, F., Trauth, M. H., & Viehberg, F. (2021). Changes in the cyclicity and variability of the eastern African paleoclimate over the last 620 kyrs. *Quaternary Science Reviews*, *273*, 107219. https://doi.org/10.1016/j.quascirev.2021.107219

Farbstein, R., & Svoboda, J. (2007). New finds of upper Palaeolithic decorative objects from Předmostí, Czech Republic. *Antiquity*, *81*(314), 856–864. https://doi.org/10.1017/S0003598X00095958

Frouin, M., Lahaye, C., Valladas, H., Higham, T., Debénath, A., Delagnes, A., & Mercier, N. (2017). Dating the middle Paleolithic deposits of La Quina Amont (Charente, France) using luminescence methods. *Journal of Human Evolution*, *109*, 30–45. https://doi.org/10.1016/j.jhevol.2017.05.002

Garcia, T., Féraud, G., Falguères, C., Lumley, H., Perrenoud, C., & Lordkipanidze, D. (2010). Earliest human remains in Eurasia: New 40Ar/ 39Ar dating of the Dmanisi hominid-bearing levels, Georgia. *Quaternary Geochronology*, *5*, 443–451. https://doi.org/10.1016/j.quageo.2009.09.012

Gower, J. C. (1975). Generalized procrustes analysis, *40*, 19–51.

Grün, R. (1996). A re-analysis of electron spin resonance dating results associated with the Petralona hominid. *Journal of Human Evolution*, *30*(3), 227–241. https://doi.org/10.1006/jhev.1996.0020

Grün, R., & Stringer, C. B. (1991). Electron spin resonance dating and the evolution of modern Humans. *Archaeometry*, *33*(2), 153–199. https://doi.org/10.1111/j.1475-4754.1991.tb00696.x

Grün, R., Pike, A., McDermott, F., Eggins, S., Mortimer, G., Aubert, M., Kinsley, L., Joannes-Boyau, R., Rumsey, M., Denys, C., Brink, J., Clark, T., & Stringer, C. (2020). Dating the skull from Broken Hill, Zambia, and its position in human evolution. *Nature*, *1–4*, 372–375. https://doi.org/10.1038/s41586-020-2165-4

Grün, R., Stringer, C., McDermott, F., Nathan, R., Porat, N., Robertson, S., Taylor, L., Mortimer, G., Eggins, S., & McCulloch, M. (2005). U-series and ESR analyses of bones and teeth relating to the human burials from Skhul. *Journal of Human Evolution*, *49*(3), 316–334. https://doi.org/10.1016/j.jhevol.2005.04.006

Grün, R., & Stringer, C. (2000). Tabun revisited: Revised ESR chronology and new ESR and U-series analyses of dental material from tabun C1. *Journal of Human Evolution*, *39*(6), 601–612. https://doi.org/10.1006/jhev.2000.0443

Grine, F. E., Bailey, R. M., Harvati, K., Nathan, R. P., Morris, A. G., Henderson, G. M., Ribot, I., & Pike, A. W. G. (2007). Late Pleistocene human skull from Hofmeyr, South Africa, and modern human origins. *Science*, *315*(5809), 226–229. https://doi.org/10.1126/science.1136294

Guérin, G., Frouin, M., Talamo, S., Aldeias, V., Bruxelles, L., Chiotti, L., Dibble, H. L., Goldberg, P., Hublin, J.-J., Jain, M., Lahaye, C., Madelaine, S., Maureille, B., McPherron, S. J. P., Mercier, N., Murray, A. S., Sandgathe, D., Steele, T. E., Thomsen, K. J., & Turq, A. (2015). A multi-method luminescence dating of the Palaeolithic sequence of La Ferrassie based on new excavations adjacent to the La Ferrassie 1 and 2 skeletons. *Journal of Archaeological Science*, *58*, 147–166. https://doi.org/10.1016/j.jas.2015.01.019

Gunz, P., Tilot, A. K., Wittfeld, K., Teumer, A., Shapland, C. Y., van Erp, T. G. M., Dannemann, M., Vernot, B., Neubauer, S., Guadalupe, T., Fernández, G., Brunner, H. G., Enard, W., Fallon, J., Hosten, N., Völker, U., Profico, A., Di Vincenzo, F., Manzi, G., … Fisher, S. E. (2019). Neandertal introgression sheds light on modern human endocranial globularity. *Current Biology*, *29*(1), 120–127.e5. https://doi.org/10.1016/j.cub.2018.10.065

Harvati, K., & Ackermann, R. R. (2022). Merging morphological and genetic evidence to assess hybridization in Western Eurasian late Pleistocene hominins. *Nature Ecology & Evolution*, *1–13*, 1573–1585. https://doi.org/10.1038/s41559-022-01875-z

Harvati, K., & Hublin, J.-J. (2012). Morphological continuity of the face in the late middle and late Pleistocene hominins from northwestern Africa: A 3D geometric morphometric analysis. In J.-J. Hublin & S. P. McPherron (Eds.), *Modern origins: A north African perspective* (pp. 179–188). Springer. https://doi.org/10.1007/978-94-007-2929-2_12

Harvati, K., & Reyes-Centeno, H. (2022). Evolution of homo in the middle and late Pleistocene. *Journal of Human Evolution*, *173*, 103279. https://doi.org/10.1016/j.jhevol.2022.103279

Head, M., & Gibbard, P. (2015). Formal subdivision of the quaternary system/period: Past, present, and future. *Quaternary International*, *383*, 4–35. https://doi.org/10.1016/j.quaint.2015.06.039

Henry-Gambier, D. (2002). Les fossiles de Cro-Magnon (Les Eyzies-de-Tayac, Dordogne). *Bulletins et mémoires de la Société d'Anthropologie de Paris*, *14*(1–2). https://doi.org/10.4000/bmsap.459

Henry-Gambier, D., Nespoulet, R., Chiotti, L., Drucker, D., & Arnaud, L. (2013). *Le Gravettien Final de l'Abri Pataud (Dordogne, France). Fouilles et Etudes 2005-2009*. Archaeopress, British Archaeological Reports, Oxford, 2458, 43–50.

Hu, W., Hao, Z., Du, P., Di Vincenzo, F., Manzi, G., Cui, J., Fu, Y.-X., Pan, Y.-H., & Li, H. (2023). Genomic inference of a severe human bottleneck during the early to middle Pleistocene transition. *Science*, *381*(6661), 979–984. https://doi.org/10.1126/science.abq7487

Hublin, J.-J. (2001). Northwestern African middle Pleistocene hominids and their bearing on the emergence of *Homo sapiens*. In L. Barham & K. Robson-Brown (Eds.), *Human roots. Africa and Asia in the middle Pleistocene*, *99–121*. CHERUB, Bristol, Western Academic and Specialist Press Ltd. https://www.academia.edu/1795661/Hublin_J.-J._2001_Northwestern_African_Middle_Pleistocene_hominids_and_their_bearing_on_the_emergence_of_Homo_sapiens._In_L._Barham_and_K._Robson-Brown_eds._Human_Roots._Africa_and_Asia_in_the_Middle_Pleistocene_99-121

Hublin, J.-J. (2013). The middle Pleistocene record. In *A companion to paleoanthropology* (pp. 517–537). John Wiley & Sons, Ltd. https://doi.org/10.1002/9781118332344.ch27

Hublin, J.-J., Ben-Ncer, A., Bailey, S. E., Freidline, S. E., Neubauer, S., Skinner, M. M., Bergmann, I., Le Cabec, A., Benazzi, S., Harvati, K., & Gunz, P. (2017). New fossils from jebel Irhoud, Morocco and the pan-African origin of *Homo sapiens*. *Nature*, *546*(7657), 289–292. https://doi.org/10.1038/nature22336

Ji, Q., Wu, W., Ji, Y., Li, Q., & Ni, X. (2021). Late middle Pleistocene Harbin cranium represents a new homo species. *The Innovation*, *2*(3). https://doi.org/10.1016/j.xinn.2021.100132

Joganic, J. L., & Heuzé, Y. (2019). Allometry and advancing age significantly structure craniofacial variation in adult female baboons. *Journal of Anatomy*, *235*(2), 217–232. https://doi.org/10.1111/joa.13005

Kaifu, Y. (2017). Archaic hominin populations in Asia before the arrival of modern humans: Their phylogeny and implications for the "southern Denisovans". *Current Anthropology*, *58*(S17), S418–S433. https://doi.org/10.1086/694318

Katz, D., & Friess, M. (2014). Technical note: 3D from standard digital photography of human crania—A preliminary assessment. *American Journal of Physical Anthropology*, *154*(1), 152–158. https://doi.org/10.1002/ajpa.22468

Katz, D. C., Grote, M. N., & Weaver, T. D. (2017). Changes in human skull morphology across the agricultural 35 transition are consistent with softer diets in preindustrial farming groups. *Proceedings of the National Academy of Sciences USA*, *114*, 9050–9055.

Kennedy, K. A. R. (2014). The application of Bayes' theorem to the Narmada cranial specimen from India: Do its morphometric features show affinity to *Homo erectus*, Neanderthals, archaic *Homo sapiens* or modern *Homo sapiens*? *Human Evolution*, *29*(4), 265283.

Klein, R. G., Avery, G., Cruz-Uribe, K., & Steele, T. E. (2007). The mammalian fauna associated with an archaic hominin skullcap and later Acheulean artifacts at Elandsfontein, Western Cape Province, South Africa. *Journal of Human Evolution*, *52*(2), 164–186. https://doi.org/10.1016/j.jhevol.2006.08.006

Klingenberg, C. P. (2002). Morphometrics and the role of the phenotype in studies of the evolution of developmental mechanisms. *Gene*, *287*(1–2), 3–10. https://doi.org/10.1016/s0378-1119(01)00867-8

Konidaris, G., Tourloukis, V., Boni, G., Athanassiou, A., Giusti, D., Thompson, N., Syrides, G., Panagopoulou, E., Karkanas, P., & Harvati, K. (2023). Marathousa 2: A New Middle Pleistocene Locality in the Megalopolis Basin (Greece) With Evidence of Hominin Exploitation of Megafauna (Hippopotamus). *PaleoAnthropology*, *1*, 34–55. https://doi.org/10.48738/2023.iss1.810

Lahr, M. M., & Foley, R. A. (1998). Towards a theory of modern human origins: Geography, demography, and diversity in recent human evolution. *American Journal of Physical Anthropology*, *107*(S27), 137–176. https://doi.org/10.1002/(SICI)1096-8644(1998)107:27+<137::AID-AJPA6>3.0.CO;2-Q

Lepre, C. J., & Kent, D. V. (2015). Chronostratigraphy of KNM-ER 3733 and other area 104 hominins from Koobi fora. *Journal of Human Evolution*, *86*, 99–111. https://doi.org/10.1016/j.jhevol.2015.06.010

Lieberman, D. E. (2011). *The Evolution of the Human Head*. Belknap Press.

Lordkipanidze, D., León, M. S. P. d., Margvelashvili, A., Rak, Y., Rightmire, G. P., Vekua, A., & Zollikofer, C. P. E. (2013). A complete skull from Dmanisi, Georgia, and the evolutionary biology of early homo. *Science*, *342*(6156), 326–331. https://doi.org/10.1126/science.1238484

Maddux, S. D., & Franciscus, R. G. (2009). Allometric scaling of infraorbital surface topography in homo. *Journal of Human Evolution*, *56*(2), 161–174. https://doi.org/10.1016/j.jhevol.2008.10.003

Manega, P. C. (1995). New geochronological results from the Ndutu, Naisiusiu and Ngaloba Beds at Olduvai and Laetoli in northern Tanzania: their significance for evolution of modern humans. In *Bellagio Conference*.

Manzi, G. (2016). Humans of the Middle Pleistocene: The controversial calvarium from Ceprano (Italy) and its significance for the origin and variability of Homo heidelbergensis. *Quaternary International*, *411*, 254–261. https://doi.org/10.1016/j.quaint.2015.12.047

Manzi, G., Magri, D., Milli, S., Palombo, M. R., Margari, V., Celiberti, V., Barbieri, M., Barbieri, M., Melis, R. T., Rubini, M., Ruffo, M., Saracino, B., Tzedakis, P. C., Zarattini, A., & Biddittu, I. (2010). The new chronology of the Ceprano calvarium (Italy). *Journal of Human Evolution*, *59*(5), 580–585. https://doi.org/10.1016/j.jhevol.2010.06.010

Margari, V., Hodell, D. A., Parfitt, S. A., Ashton, N. M., Grimalt, J. O., Kim, H., Yun, K.-S., Gibbard, P. L., Stringer, C. B., Timmermann, A., & Tzedakis, P. C. (2023). Extreme glacial cooling likely led to hominin depopulation of Europe in the early Pleistocene. *Science (New York, N.Y.)*, *381*(6658), 693–699. https://doi.org/10.1126/science.adf4445

Marra, F., Ceruleo, P., Jicha, B., Pandolfi, L., Petronio, C., & Salari, L. (2015). A new age within MIS 7 for the homo neanderthalensis of Saccopastore in the glacio-eustatically forced sedimentary successions of the Aniene River valley, Rome. *Quaternary Science Reviews*, *129*, 260–274. https://doi.org/10.1016/j.quascirev.2015.10.027

Matsu'ura, S., Kondo, M., Danhara, T., Sakata, S., Iwano, H., Hirata, T., Kurniawan, I., Setiyabudi, E., Takeshita, Y., Hyodo, M., Kitaba, I., Sudo, M., Danhara, Y., & Aziz, F. (2020). Age control of the first appearance datum for Javanese Homo erectus in the Sangiran area. *Science*, *367*(6474), 210–214. https://doi.org/10.1126/science.aau8556

Meyer, M., Arsuaga, J.-L., de Filippo, C., Nagel, S., Aximu-Petri, A., Nickel, B., Martínez, I., Gracia, A., Bermúdez de Castro, J. M., Carbonell, E., Viola, B., Kelso, J., Prüfer, K., & Pääbo, S. (2016). Nuclear DNA sequences from the middle Pleistocene Sima de los Huesos hominins. *Nature*, *531*(7595), 504–507. https://doi.org/10.1038/nature17405

Meyer, M., Fu, Q., Aximu-Petri, A., Glocke, I., Nickel, B., Arsuaga, J.-L., Martínez, I., Gracia, A., de Castro, J. M. B., Carbonell, E., & Pääbo, S. (2014). A mitochondrial genome sequence of a hominin from Sima de los Huesos. *Nature*, *505*(7483), 403–406. https://doi.org/10.1038/nature12788

Mirazón Lahr, M. (2016). The shaping of human diversity: Filters, boundaries and transitions. *Philosophical Transactions of the Royal Society B: Biological Sciences*, *371*(1698), 20150241. https://doi.org/10.1098/rstb.2015.0241

Mitteroecker, P. (2020). Morphometrics in evolutionary developmental biology. In L. N. de la Rosa & G. Müller (Eds.), *Evolutionary Developmental Biology*(pp. 1–11). Springer, Cham. https://doi.org/10.1007/978-3-319-33038-9_119-1

Moghimbeygi, M., & Nodehi, A. (2022). Multinomial principal component logistic regression on shape data. *Journal of Classification*, *39*, 578–599. https://doi.org/10.1007/s00357-022-09423-x

Moncel, M.-H., Despriée, J., Courcimaut, G., Voinchet, P., & Bahain, J.-J. (2020). La Noira site (Centre, France) and the technological Behaviours and skills of the earliest Acheulean in Western Europe between 700 and 600 ka. *Journal of Paleolithic Archaeology*, *3*(3), 255–301. https://doi.org/10.1007/s41982-020-00049-2

Moncel, M.-H., Santagata, C., Pereira, A., Nomade, S., Voinchet, P., Bahain, J.-J., Daujeard, C., Curci, A., Lemorini, C., Hardy, B., Eramo, G., Berto, C., Raynal, J.-P., Arzarello, M., Mecozzi, B., Iannucci, A., Sardella, R., Allegretta, I., Delluniversità, E., … Piperno, M. (2020). The origin of early Acheulean expansion in Europe 700 ka ago: New findings at Notarchirico (Italy). *Scientific Reports*, *10*(1), 13802. https://doi.org/10.1038/s41598-020-68617-8

Mounier, A. (2009). Validité du taxon *Homo heidelbergensis* Schoetensack, 1908. [These de doctorat, Aix-Marseille 2]. https://paleoanthro.org/media/dissertations/M_Aurelien_Mounier.pdf, http://www.theses.fr/fr/2009AIX20693

Mounier, A. (2011). Définition du taxon *Homo heidelbergensis* Schoetensack, 1908: analyse phénétique du massif facial supérieur des fossiles du genre Homo du Pléistocène moyen. *Bulletins et Mémoires de la Société d'Anthropologie de Paris*, *23*(3), 115–151. https://doi.org/10.1007/s13219-011-0038-y

Mounier, A. (2012). Le massif facial supérieur d'*Homo heidelbergensis* Schoetensack, 1908: l'apport de la morphométrie géométrique. *Bulletins et Mémoires de la Société d'Anthropologie de Paris*, *24*, 51–68. https://doi.org/10.1007/s13219-011-0041-3

Mounier, A., Condemi, S., & Manzi, G. (2011). The stem species of our species: A place for the archaic human cranium from Ceprano, Italy. *PLoS One*, *6*(4), e18821. https://doi.org/10.1371/journal.pone.0018821

Mounier, A., Correia, M., Rivera, F., Crivellaro, F., Power, R., Jeffery, J., Wilshaw, A., Foley, R. A., & Mirazón Lahr, M. (2018). Who were the Nataruk people? Mandibular morphology among late Pleistocene and early Holocene fisher-forager populations of West Turkana (Kenya). *Journal of Human Evolution.*, *121*, 235–253. https://doi.org/10.1016/j.jhevol.2018.04.013

Mounier, A., Marchal, F., & Condemi, S. (2009). Is *Homo heidelbergensis* a distinct species? New insight on the Mauer mandible. *Journal of Human Evolution*, *56*(3), 219–246. https://doi.org/10.1016/j.jhevol.2008.12.006

Mounier, A., & Caparros, M. (2015). Le statut phylogénétique d'*Homo heidelbergensis* – étude cladistique des homininés du Pléistocène moyen. *BMSAP*, *27*(3), 110–134. https://doi.org/10.1007/s13219-015-0127-4

Mounier, A., & Mirazón Lahr, M. (2016). Virtual ancestor reconstruction: Revealing the ancestor of modern humans and Neandertals. *Journal of Human Evolution*, *91*, 57–72. https://doi.org/10.1016/j.jhevol.2015.11.002

Mounier, A., & Mirazón Lahr, M. (2019). Deciphering African late middle Pleistocene hominin diversity and the origin of our species. *Nature Communications*, *10*(1), 3406. https://doi.org/10.1038/s41467-019-11213-w

Nathan, R. P. (2010). Numerical modelling of environmental dose rate and its application to trapped-charge dating, Ph.D. Thesis, University of Oxford. http://ora.ox.ac.uk/objects/uuid:3da656e8-5514-4fed-85d1-8664e5dc1932

Ni, X. (2021). Massive cranium from Harbin in northeastern China establishes a new middle Pleistocene human lineage, *2*, 256.

Petr, M., Hajdinjak, M., Fu, Q., Essel, E., Rougier, H., Crevecoeur, I., Semal, P., Golovanova, L. V., Doronichev, V. B., Lalueza-Fox, C., de la Rasilla, M., Rosas, A., Shunkov, M. V., Kozlikin, M. B., Derevianko, A. P., Vernot, B., Meyer, M., & Kelso, J. (2020). The evolutionary history of Neanderthal and Denisovan Y chromosomes. *Science*, *369*(6511), 1653–1656. https://doi.org/10.1126/science.abb6460

Pettitt, P. B., & Trinkaus, E. (2000). Direct radiocarbon dating of the BRNO 2 gravettian human remains, *38*(2), 149–150.

Pomeroy, E., Bennett, P., Hunt, C. O., Reynolds, T., Farr, L., Frouin, M., Holman, J., Lane, R., French, C., & Barker, G. (2020). New Neanderthal remains associated with the 'flower burial' at Shanidar cave. *Antiquity*, *94*(373), 11–26. https://doi.org/10.15184/aqy.2019.207

Posth, C., Wißing, C., Kitagawa, K., Pagani, L., van Holstein, L., Racimo, F., Wehrberger, K., Conard, N. J., Kind, C. J., Bocherens, H., & Krause, J. (2017). Deeply divergent archaic mitochondrial genome provides lower time boundary for African gene flow into Neanderthals. *Nature Communications*, *8*(1), 1–9. https://doi.org/10.1038/ncomms16046

Reich, D., Green, R. E., Kircher, M., Krause, J., Patterson, N., Durand, E. Y., Viola, B., Briggs, A. W., Stenzel, U., Johnson, P. L. F., Maricic, T., Good, J. M., Marques-Bonet, T., Alkan, C., Fu, Q., Mallick, S., Li, H., Meyer, M., Eichler, E. E., … Pääbo, S. (2010). Genetic history of an archaic hominin group from Denisova cave in Siberia. *Nature*, *468*(7327), 1053–1060. https://doi.org/10.1038/nature09710

Richter, D., Grün, R., Joannes-Boyau, R., Steele, T., Amani, F., Rué, M., Fernandes, P., Raynal, J.-P., Geraads, D., Ben-Ncer, A., Hublin, J.-J., & Mcpherron, S. (2017). The age of the hominin fossils from jebel Irhoud, Morocco, and the origins of the middle stone age. *Nature*, *546*, 293–296. https://doi.org/10.1038/nature22335

Rightmire, G. P. (1983). The Lake Ndutu cranium and early homo sapiens in Africa. *American Journal of Physical Anthropology*, *61*(2), 245–254. https://doi.org/10.1002/ajpa.1330610214

Rightmire, G. P. (1998). Human evolution in the middle Pleistocene: The role of *Homo heidelbergensis*. *Evolutionary Anthropology: Issues, News, and Reviews*, *6*(6), 218–227. https://doi.org/10.1002/(SICI)1520-6505(1998)6:6<218::AID-EVAN4>3.0.CO;2-6

Rightmire, G. P. (2001). Patterns of hominid evolution and dispersal in the middle Pleistocene. *Quaternary International*, *75*(1), 77–84. https://doi.org/10.1016/S1040-6182(00)00079-3

Rightmire, G. P. (2008). Homo in the middle pleistocene: Hypodigms, variation, and species recognition. *Evolutionary Anthropology: Issues, News, and Reviews*, *17*(1), 8–21. https://doi.org/10.1002/evan.20160

Rightmire, G. P. (2015). Later Middle Pleistocene Homo. In W. Henke & I. Tattersall (Eds.), *Handbook of paleoanthropology* (pp. 2221–2242). Springer. https://doi.org/10.1007/978-3-642-39979-4_55

Rightmire, G. P. (2017). Middle Pleistocene homo crania from Broken Hill and Petralona: Morphology, metric comparisons, and evolutionary relationships. In A. Marom & E. Hovers (Eds.), *Human paleontology and prehistory: Contributions in honor of Yoel Rak* (p. 145159). Springer International Publishing. https://doi.org/10.1007/978-3-319-46646-0_11

Rizal, Y., Westaway, K. E., Zaim, Y., van den Bergh, G. D., Bettis, E. A., Morwood, M. J., Huffman, O. F., Grün, R., Joannes-Boyau, R., Bailey, R. M., Sidarto, Westaway, M. C., Kurniawan, I., Moore, M. W., Storey, M., Aziz, F., Suminto, Zhao, J., Aswan, Sipola, M. E., Larick, R., Zonneveld, J.-P., Scott, R., Putt, S., Ciochon, R. L. (2020). Last appearance of *Homo erectus* at Ngandong, Java, 117,000–108,000 years ago. *Nature*, *577*(7790), 381–385. https://doi.org/10.1038/s41586-019-1863-2

Rohlf, F. J., & Slice, D. (1990). Extensions of the procrustes method for the optimal superimposition of landmarks. *Systematic Zoology*, *39*(1), 40–59. https://doi.org/10.2307/2992207

Roksandic, M., Radović, P., Wu, X.-J., & Bae, C. J. (2022). Resolving the "muddle in the middle": The case for Homo bodoensis sp. nov. *Evolutionary Anthropology: Issues, News, and Reviews*, *31*(1), 20–29. https://doi.org/10.1002/evan.21929

Rosenberg, K. R., Zuné, L., & Ruff, C. B. (2006). Body size, body proportions, and encephalization in a middle Pleistocene archaic human from northern China. *Proceedings of the National Academy of Sciences*, *103*(10), 3552–3556. https://doi.org/10.1073/pnas.0508681103

Sankhyan, A. R. (2020). Evolutionary perspective on Narmada hominin fossils. *Advances in Anthropology*, *10*(3), 235–258. https://doi.org/10.4236/aa.2020.103013

Schlager, S. (2017). Chapter 9: Morpho and Rvcg – Shape analysis in R: R-packages for geometric morphometrics, shape analysis and surface manipulations. In G. Zheng, S. Li, & G. Székely (Eds.), *Statistical shape and deformation analysis* (pp. 217–256). Academic Press. https://doi.org/10.1016/B978-0-12-810493-4.00011-0

Schlebusch, C. M., Malmström, H., Günther, T., Sjödin, P., Coutinho, A., Edlund, H., Munters, A. R., Vicente, M., Steyn, M., Soodyall, H., Lombard, M., & Jakobsson, M. (2017). Southern African ancient genomes estimate modern human divergence to 350,000 to 260,000 years ago. *Science*, *358*(6363), 652–655. https://doi.org/10.1126/science.aao6266

Schlebusch, C. M., Sjödin, P., Breton, G., Günther, T., Naidoo, T., Hollfelder, N., Sjöstrand, A. E., Xu, J., Gattepaille, L. M., Vicente, M., Scofield, D. G., Malmström, H., de Jongh, M., Lombard, M., Soodyall, H., & Jakobsson, M. (2020). Khoe-san genomes reveal unique variation and confirm the deepest population divergence in *Homo sapiens*. *Molecular Biology and Evolution*, *37*(10), 2944–2954. https://doi.org/10.1093/molbev/msaa140

Schmitz, R. W., Serre, D., Bonani, G., Feine, S., Hillgruber, F., Krainitzki, H., Pääbo, S., & Smith, F. H. (2002). The Neandertal type site revisited: Interdisciplinary investigations of skeletal remains from the Neander Valley, Germany. *Proceedings of the National Academy of Sciences*, *99*(20), 13342–13347. https://doi.org/10.1073/pnas.192464099

Schwarcz, H. P., Grün, R., Vandermeersch, B., Bar-Yosef, O., Valladas, H., & Tchernov, E. (1988). ESR dates for the hominid burial site of Qafzeh in Israel. *Journal of Human Evolution*, *17*(8), 733–737. https://doi.org/10.1016/0047-2484(88)90063-2

Shen, G., Gao, X., Gao, B., & Granger, D. E. (2009). Age of Zhoukoudian *Homo erectus* determined with 26 Al/ 10 Be burial dating. *Nature*, *458*(7235), 198–200. https://doi.org/10.1038/nature07741

Slizewski, A., Friess, M., & Semal, P. (2010). Surface scanning of anthropological specimens: Nominal-actual comparison with low cost laser scanner and high end fringe light projection surface scanning systems Oberflächenscannen anthropologischer Objekte: Soll-Ist Vergleiche mit einem niedrigpreisigen Laserscanner und hochpreisigen Streifenlicht. https://www.semanticscholar.org/paper/Surface-scanning-of-anthropological-specimens%3A-with-Slizewski-Friess/9cb0eb843680ed90ea9312418931de8615175334

Smith, H. F. (2009). Which cranial regions reflect molecular distances reliably in humans? Evidence from three8 dimensional morphology. *American Journal of Human Biology*, *21*, 36–47.

Stringer, C. (2002). Modern human origins: Progress and prospects. *Philosophical Transactions of the Royal Society of London. Series B: Biological Sciences*, *357*(1420), 563–579. https://doi.org/10.1098/rstb.2001.1057

Stringer, C. (2012). The status of *Homo heidelbergensis* (Schoetensack 1908). *Evolutionary Anthropology: Issues, News, and Reviews*, *21*(3), 101–107. https://doi.org/10.1002/evan.21311

Stringer, C. B. (1983). Some further notes on the morphology and dating of the Petralona hominid. *Journal of Human Evolution*, *12*(8), 731–742. https://doi.org/10.1016/S0047-2484(83)80128-6

Svoboda, J., Novák, M., Sázelová, S., & Demek, J. (2016). Pavlov I: A large Gravettian site in space and time. *Quaternary International*, *406*, 95–105. https://doi.org/10.1016/j.quaint.2015.09.015

Tamrat, E., Thouveny, N., Taïeb, M., & Opdyke, N. D. (1995). Revised magnetostratigraphy of the Plio-Pleistocene sedimentary sequence of the Olduvai formation (Tanzania). *Palaeogeography, Palaeoclimatology, Palaeoecology*, *114*(2), 273–283. https://doi.org/10.1016/0031-0182(94)00080-R

Tattersall, I. (2011). Before the Neanderthals: Hominid evolution in middle Pleistocene Europe. *Vertebrate Paleobiology and Paleoanthropology*, 47–53. https://doi.org/10.1007/978-94-007-0492-3_4

Tourloukis, V., & Harvati, K. (2018). The Palaeolithic record of Greece: A synthesis of the evidence and a research agenda for the future. *Quaternary International*, *466*, 48–65. https://doi.org/10.1016/j.quaint.2017.04.020

Tsakanikou, P., Galanidou, N., & Sakellariou, D. (2020). Lower Palaeolithic archaeology and submerged landscapes in Greece: The current state of the art. *Quaternary International.*, *584*, 171–181. https://doi.org/10.1016/j.quaint.2020.05.025

Valladas, H., Mercier, N., Froget, L., Hovers, E., Joron, J.-L., Kimbel, W. H., & Rak, Y. (1999). TL dates for the Neanderthal site of the Amud cave, Israel. *Journal of Archaeological Science*, *26*(3), 259–268. https://doi.org/10.1006/jasc.1998.0334

Venables, B., & Ripley, B. (2002). *Modern applied statistics with S*. Springer. https://doi.org/10.1007/b97626

Vidal, C. M., Lane, C. S., Asrat, A., Barfod, D. N., Mark, D. F., Tomlinson, E. L., Tadesse, A. Z., Yirgu, G., Deino, A., Hutchison, W., Mounier, A., & Oppenheimer, C. (2022). Age of the oldest known *Homo sapiens* from eastern Africa. *Nature*, *15*, 579–583. https://doi.org/10.1038/s41586-021-04275-8

von Cramon-Taubadel, N. (2009). Congruence of individual cranial bone morphology and neutral molecular 27 affinity patterns in modern humans. *American Journal of Physical Anthropology*, *140*, 205–215.

Waltenberger, L., Rebay-Salisbury, K., & Mitteroecker, P. (2021). Three-dimensional surface scanning methods in osteology: A topographical and geometric morphometric comparison. *American Journal of Physical Anthropology*, *174*(4), 846–858. https://doi.org/10.1002/ajpa.24204

Wild, E. M., Teschler-Nicola, M., Kutschera, W., Steier, P., Trinkaus, E., & Wanek, W. (2005). Direct dating of early upper Palaeolithic human remains from Mladeč. *Nature*, *435*(7040), 332–335. https://doi.org/10.1038/nature03585

Wu, X.-J., Pei, S.-W., Cai, Y.-J., Tong, H.-W., Li, Q., Dong, Z., Sheng, J.-C., Jin, Z.-T., Ma, D.-D., Xing, S., Li, X.-L., Cheng, X., Cheng, H., de la Torre, I., Edwards, R. L., Gong, X.-C., An, Z.-S., Trinkaus, E., & Liu, W. (2019). Archaic human remains from Hualongdong, China, and middle Pleistocene human continuity and variation. *Proceedings of the National Academy of Sciences*, *116*(20), 9820–9824. https://doi.org/10.1073/pnas.1902396116

Xiao, J., Jin, C., & Zhu, Y. (2002). Age of the fossil Dali man in north-central China deduced from chronostratigraphy of the loess–paleosol sequence. *Quaternary Science Reviews*, *21*(20), 2191–2198. https://doi.org/10.1016/S0277-3791(02)00011-2

Zaidi, A. A., Mattern, B. C., Claes, P., McEcoy, B., Hughes, C., & Shriver, M. D. (2017). Investigating the case of 43 human nose shape and climate adaptation. *PLoS Genetics*, *13*, e1006616.

SUPPORTING INFORMATION

Additional supporting information can be found online in the Supporting Information section at the end of this article.

How to cite this article: Hautavoine, H., Arnaud, J., Balzeau, A., & Mounier, A. (2024). Quantifying hominin morphological diversity at the end of the middle Pleistocene: Implications for the origin of *Homo sapiens*. *American Journal of Biological Anthropology*, *184*(2), e24915. https://doi.org/10.1002/ajpa.24915